

# High-Resolution Spectroscopy of FUors

G. H. Herbig

*Institute for Astronomy, University of Hawaii,  
2680 Woodlawn Drive, Honolulu, Hawaii 96822, U.S.A.*

P. P. Petrov

*Crimean Astrophysical Observatory, p/o Nauchny, Crimea 98409, Ukraine  
and*

R. Duemmler<sup>1</sup>

*Astronomy Division, University of Oulu, P.O. Box 3000, FIN-90014, Finland*

## ABSTRACT

High-resolution spectroscopy was obtained of the FUors FU Ori and V1057 Cyg between 1995 and 2002 with the SOFIN spectrograph at NOT and with HIRES at Keck I. During these years FU Ori remained about 1 mag. (in B) below its 1938–39 maximum brightness, but V1057 Cyg (B ≈ 10.5 at peak in 1970–71) faded from about 13.5 to 14.9 and then recovered slightly. Their photospheric spectra resemble that of a rotationally broadened, slightly veiled supergiant of about type G0 Ib, with  $v_{\text{eq}} \sin i = 70 \text{ km s}^{-1}$  for FU Ori, and  $55 \text{ km s}^{-1}$  for V1057 Cyg. As V1057 Cyg faded, P Cyg structure in H $\alpha$  and the IR Ca II lines strengthened, and a complex shortward-displaced shell spectrum of low-excitation lines of the neutral metals (including Li I and Rb I) increased in strength, disappeared in 1999, and reappeared in 2001. Several SOFIN runs extended over a number of successive nights so that a search for rapid and cyclic changes in the spectra was possible. These spectra show rapid night-to-night changes in the wind structure of FU Ori at H $\alpha$ , including clear evidence of sporadic infall. The equivalent width of the P Cyg absorption varied cyclically with a period of 14.8 days, with phase stability maintained over 3 seasons. This is believed to be the rotation period of FU Ori. The internal structure of its photospheric lines also varies cyclically, but with a period of 3.54 days. A similar variation may be present in V1057 Cyg, but the data are much noisier and that result uncertain. As V1057 Cyg has faded and the continuum level fallen, the emission lines of a pre-existing low-excitation chromosphere have emerged. Therefore we believe that the ‘line doubling’ in V1057 Cyg is produced by these central emission cores in the absorption lines, not by orbital motion in an inclined Keplerian disk. No dependence of  $v_{\text{eq}} \sin i$  on wavelength or excitation potential was detected in either FU Ori or V1057 Cyg, again contrary to expectation for a self-luminous accretion disk. It was found also that certain critical lines in the near infrared are not accounted for by synthetic disk spectra. It is concluded that a rapidly rotating star near the edge of stability, as proposed by Larson (1980), can better account for these observations. The possibility is also considered that FUor eruptions are not a property of ordinary T Tauri stars, but may be confined to a special sub-species of rapidly rotating pre-main sequence stars having powerful quasi-permanent winds.

*Subject headings:* stars: evolution — stars: Pre-Main-Sequence — stars: individual (FU Ori, V1057 Cyg)

## 1. Introduction

The variable star now known as FU Ori was originally believed to be a slow nova because of its leisurely rise from  $m_{pg} = 16$  to 10 over an interval of about a year in 1937–39. There were some misgivings at the time about that classification: the spectrum was quite unlike that of an ordinary nova, and for a nova the star was most unusually located in the dark cloud Barnard 35, itself in the OB association surrounding  $\lambda$  Ori. It is now realized that FU Ori is no nova, but represents another phenomenon altogether. It is the prototype of a small class of pre-main sequence objects, named ‘FUors’ by Ambartsumian, that have received an increasing amount of attention over the past three decades.

Three additional stars, and possibly 2 more, now collectively define the FUor class on the grounds of a well-documented major rise in brightness, association with a molecular cloud, and a spectrum like that of FU Ori. These ‘classical FUors’ are V1057 Cyg, V1515 Cyg, V1735 Cyg, probably V346 Nor (Reipurth 1990), and possibly a star (CB34V = V1184 Tau) discussed most recently by Alves et al. (1997). A number of other pre-main sequence stars have been proposed for membership, usually on the grounds of spectroscopic resemblance plus an infrared excess, but none have been observed to brighten up and remain so for years, as did the classical FUors mentioned above.

The time seems appropriate for a reexamination of the observational situation for two reasons. First, the other classical FUors remain not far from their maximum brightness, but V1057 Cyg has faded about 4 mag. (in B) since 1971.

Second, high-resolution spectroscopy has now become feasible for all FUors over a wider wavelength range (3500–9000 Å) than was heretofore possible, and in the case of V1057 Cyg almost on an annual basis. The observations to be discussed here have been obtained by Petrov and collaborators with the SOFIN echelle spectrograph (Tuominen, Ilyin, & Petrov 1990) of the Nordic Optical telescope at La Palma<sup>2</sup> between 1996 and 2002 at

a resolution of about 13 km s<sup>−1</sup>; and by Herbig with the HIRES echelle at the Keck I telescope on Mauna Kea<sup>3</sup> since 1996 at a resolution of about 7 km s<sup>−1</sup>. Several of the SOFIN runs extended over a number of successive nights, offering the opportunity to search for rapid changes in the spectra.<sup>4</sup> Some of the SOFIN material has already been discussed by Petrov et al. (1998) and by Laakkonen (2000). We here expand upon those results.

It is now accepted that FUors represent an interesting phenomenon of early stellar evolution, but it is uncertain how universal it is, and there is disagreement on what is responsible for the outbursts. Hypotheses as to the latter fall into two classes: Hartmann, Kenyon, and their colleagues have proposed that the flare-up is a phenomenon not of the pre-outburst star itself, but is the result of a major increase in the surface brightness of the circumstellar accretion disk. Since the idea was first put forward by Hartmann & Kenyon (1985, hereafter HK), it has been elaborated extensively Hartmann & Kenyon (and reviewed: 1996). Building upon that proposition, theories of instabilities intrinsic to such an accretion disk have been examined by Clarke, Lin, & Pringle (1990), by Kley & Lin (1999) and by Bell (1999, which contains references to earlier papers).

The opposite hypothesis is that the star itself is responsible for the FUor flare-up. The absorption lines in the classical FUors are broad; if they are the result of axial rotation in a spherical limb-darkened star, fits to the optical-region line profiles (§ 4.2, below) yield values of  $v_{eq} \sin i$  up to about 70 km s<sup>−1</sup> in the case of FU Ori. A periodic modulation of the line structure of FU Ori (described in § 4.4) leads to a radius of the order of  $20 \sin i R_\odot$ . Given those parameters, the condition that FU Ori be rotationally stable (in the sense that the centrifugal acceleration at the equator of a oblate rotator equals the gravitational

and Sweden, in the Spanish Observatorio del Roque de los Muchachos of the Instituto de Astrofísica de Canarias.

<sup>3</sup>The W. M. Keck Observatory is operated as a scientific partnership among the California Institute of Technology, the University of California, and the National Aeronautics and Space Administration. The Observatory was made possible by the generous financial support of the W. M. Keck Foundation.

<sup>4</sup>The dates of the SOFIN observations are not tabulated here, but can be retrieved from the listing in Table 9, this paper.

[Porter 1996]) is  $(M/M_{\odot}) \sin i > 0.79$ . Clearly, a not-unreasonable value of  $\sin i$  would require a substantial stellar mass to ensure the stability of such a rapid rotator.

An examination by Larson (1980) of the consequences of such very rapid rotation suggested that bar-like deformations would develop that could produce heating of the outer layers of the star, thus accounting for the flare-up and mass loss. One would think that such instabilities might produce detectable photometric variation with the rotation period. The only search for such variations is that reported for FU Ori by Kenyon et al. (2000). They found only ‘random’ fluctuations of amplitude 3-4% on time scales of 1 day or less, but it would be worthwhile to repeat such observations with better time coverage. Later (§ 4.4) we describe the results of a search for cyclic variations in radial velocity and line structure in both FU Ori and V1057 Cyg.

Little more has been heard of the rapid-rotator hypothesis, perhaps because of the appeal of the disk-instability idea and the volume of publication that it has engendered. But on earlier occasions we have pointed out some difficulties and our reservations about the HK proposal (Herbig 1989; Petrov & Herbig 1992). The theory was subsequently modified to explain one of those concerns Bell et al. (1995). However the new results to be described here call into question the original observational justification for the HK hypothesis, on which that theory is based. In the following sections we examine three issues that have been regarded as crucial support for that hypothesis:

(a) The ‘doubling’ of certain absorption lines is evidence of Keplerian motion in an inclined disk (§ 2.4);

(b) A dependence on  $v_{\text{eq}} \sin i$  on wavelength or excitation potential in the optical region up to 9000 Å is evidence of the decline in orbital velocity with radius expected under the disk hypothesis (§ 4.2); and

(c) The theoretical disk spectrum, as a composite of annuli of temperature and surface brightness that decline with distance from the center, fits the observed spectra of FUors (§ 4.1).

When V1057 Cyg was bright, it was noticed that the spectral type became later with increasing wavelength across the optical region. The ef-

fect became striking when observations were extended to the near-IR (Mould et al. 1978; Elias 1978) and H<sub>2</sub>O and CO bands were found in the spectrum of an ostensible F- or G-type star. No evidence of radial velocity variation with time or with wavelength has been reported, so the spectrum apparently originates in a single object. The disk hypothesis does have the persuasive advantage of explaining, although not in detail (§ 4.1), this apparently composite nature of FUor spectra as the falloff of temperature with increasing radius in an accretion disk.

But it is now realized that the simple presence of the 2.3-μm CO bands in a G supergiant is not that unusual (Wallace & Hinkle 1997). They appear at about G0 Ib and are prominent by G8 Ib, although in FU Ori and V1057 Cyg they are as strong as in early M-type. It would be interesting to investigate if such an effect could be simulated in an extended envelope around a rapidly rotating single star.

We are not necessarily committed to the concept of an unstable rapid rotator as a final solution to the FUor phenomenon. But for lack of a more persuasive alternative, in what follows we examine the observational information in terms of that hypothesis. First we describe the spectrum of V1057 Cyg during its 1996–2002 fading, the period for which we have detailed high-resolution coverage (§ 2), followed by a discussion of its light curve (§ 3), and then we review the spectroscopic properties of FUors in general (§ 4).

## 2. The Spectrum of V1057 Cyg 1996–2002

Figure 1 shows the B/pg light curve of V1057 Cyg. Most of the high-resolution spectra of V1057 Cyg discussed in the literature were obtained in the 1980’s, when the star was descending to a plateau of brightness between about B = 13.0 and 13.3, which extended from 1985 to about 1994. Between 1994 and 1995 it began to fade again, and reached a minimum near 14.9 in 1999, since which it has recovered slightly. Briefly, following Petrov et al. (1998) and Laakkonen (2000), this is what happened in the spectrum during the post-1994 minimum with respect to the 1980s:

the photospheric lines became much shallower, some with pronounced emission cores;

the P Cyg absorptions in  $H\alpha$ , infrared Ca II and other lines became stronger;

the shortward-shifted shell components in the low excitation lines increased in strength

(1996-97), then essentially disappeared (1999), but reappeared in 2001;

TiO bands in the expanding shell appeared for the first time, and

a number of emission lines of low excitation appeared in the spectrum.

## 2.1. Photospheric spectrum

Simple inspection of the absorption spectrum of V1057 Cyg shows that it resembles that of a rotationally broadened early-G supergiant. To make this quantitative, the excitation temperature and gravity were determined as follows. Equivalent widths (hereafter abbreviated EW) were measured for 30 of the least blended photospheric lines of Fe I in the region 4950-8000 Å (shell components, which could distort the measurements, were almost absent in this spectral region in 1998-1999). The curve of growth gives  $T_{exc} = 5300 \pm 300$  K. The single measurable line of Fe II,  $\lambda 5991$ , lies on this curve at a position corresponding to  $\log n_e = 12$ . These are indeed values expected for a G1 supergiant. Furthermore, a comparison of V1057 Cyg with templates of 41 Cyg (F5 II),  $\beta$  Aqr (G0 Ib), 9 Peg (G5 Ib) and 40 Peg (G8 II) show that the line ratios correspond to F7-G3 I-II.

The photospheric absorption lines in August 1997 appeared to be shallower than in the spectra found in the literature. Many of the lower-excitation lines appear double, as the result of what is clearly an emission component at the bottom of the absorption. With respect to spectra of the 1980's, this line 'doubling,' measured as a velocity separation between the two absorption minima, had increased by October 1996, and even more by August 1997, as the result of what is clearly an emission component appearing at the bottom of the absorption line (see § 2.4). However, the line width of the absorptions near the continuum level remains the same as in the spectra taken, e.g., in 1983-84 by Kenyon, Hartmann, & Hewett (1988) and in 1992 by Hartmann & Calvet (1995). That is, the overall line width has not changed, but in those where the central reversal has become more prominent the line depth has been reduced. In

this way many photospheric lines appear significantly shallower than in the accretion disk model of Kenyon et al. (1988), which was designed to fit the spectrum of V1057 Cyg in 1985 (Fig. 13).

However, there is another effect as well: in the red, higher-excitation lines where no central emission is expected are also shallower than in the spun-up standards, as if a veiling continuum is superposed upon the absorption spectrum. Veiling factors of 0.3 to 0.5 are indicated.

## 2.2. Wind/P Cyg Features

Table 1 gives the parameters of the P Cyg structure at  $H\alpha$  as measured on all spectra either published or our own. One sees that the mass-loss in the wind of V1057 Cyg, as evidenced by the strength of the P Cyg absorption component at  $H\alpha$ , began to increase about 1984-85 (Laakonen 2000), near the beginning of the photometric plateau. It is tempting to speculate that the two may be connected. Earlier, the P Cyg absorption of  $H\alpha$  was not saturated and its structure varied considerably at all velocities (Croswell, Hartmann, & Avrett 1987, and Table 1). During the post-plateau minimum (i.e., after 1994-95) the line remained strong, but the high velocity wing (-200 to -400 km s<sup>-1</sup>) varied in depth from year to year while the low velocity section (-60 to -120 km s<sup>-1</sup>) always remained deep (Figs. 7, 24).

The only known observations of  $H\alpha$  during the plateau decade are those obtained in 1988 by Welty et al. (1992) and by Budge (unpublished). Those entries in Table 1 have been measured from their profiles. The EW of the P Cyg absorption component in that year was the largest that has been reported. No other observations of  $H\alpha$  are known to have been made during 1986-95, but Rustamov (2001) measured the structure of  $H\beta$  and  $H\gamma$  between 1978 and 1990 (photographically and at a resolution of about 1000). His data indicate that the EW of  $H\beta$  declined from 1978 to 1985 but had increased again by 1987 (no observation in 1986), continued to increase thereafter and by 1990 was the largest he had observed.

The lack of adequate spectroscopic coverage of V1057 Cyg during the 1986-95 decade is regrettable.

Figure 2 shows the P Cyg profiles of the  $H\alpha$ ,  $H\beta$ , Na I and Ca II  $\lambda 8542$  lines on the 1997 August

SOFIN spectrogram. (Throughout we denote the measured (heliocentric) velocity of a features as  $v$  and the stellar velocity as  $v_*$ , so velocity in the star's rest frame is  $RV = v - v_*$ .) The  $H\alpha$  profile is similar to that of FU Ori, where the mass-loss rate was estimated to be an order of magnitude larger than in V1057 Cyg in 1985 (Croswell et al. 1987).

### 2.3. Shell Features

The low excitation ( $<1$  eV) photospheric absorption lines of V1057 Cyg have almost always been flanked shortward by narrow, often complex 'shell' features. They are prominent in the strong low-excitation lines of the neutral metals at shorter wavelengths. They are probably due to condensations in the expanding wind passing in front of the star. In 1996, by which time the star had faded by about 1 mag. (in B) from plateau brightness, both the P Cyg absorption at the Balmer lines and the shell lines had become stronger, to such a degree that the shell also became detectable at many lines in the red.

Figure 3 shows some shell line profiles at the  $13 \text{ km s}^{-1}$  SOFIN resolution. The underlying photospheric spectrum has been subtracted, as described later (§ 2.5). The strong lines of higher excitation potential (hereafter EP), as Mg I  $\lambda 5183$  and Fe II  $\lambda 5316$ , also contain shortward shell components but at more negative velocities, about  $-120 \text{ km s}^{-1}$ . These absorptions are much broader than those at the low excitation lines, and so represent an intermediate case between shell and wind.

Another indicator of a cool expanding shell are the numerous TiO bands (Fig. 4). All the TiO bands were blue-shifted to  $RV = -40$  to  $-70 \text{ km s}^{-1}$ ; i.e. to about the same velocity as the shell components of low excitation lines. These shell lines and the TiO bands in the red were strongest in 1996, weaker in 1997, and absent in 1998, 1999 and 2000. By 2001 the shell lines and TiO bands had reappeared, but with somewhat broader profiles and larger expansion velocities (see Fig. 3, bottom).

The complexity of the shell structure is more apparent at HIRES resolution, where at least five separate components are seen. The shell was so prominent in 1996–97 at low-level lines of neutral

metals (Al I, Fe I, Ti I, Cr I, Mn I), as well as in Ba II, Li I, and Rb I as to confuse the shortward wings of the underlying stellar features. The 4990–5020 Å region, containing a number of prominent Ti I lines, is shown in Figure 5. At the top of the figure is the same section in the G5 Ib star HD 190113, as broadened by  $v_{\text{eq}} \sin i = 55 \text{ km s}^{-1}$ , to represent the underlying photospheric spectrum.

At that time (1997 Aug. 12–13), the shell lines were at velocities of  $-128$ ,  $-107$ ,  $-89$ ,  $-78$ , and  $-61 \text{ km s}^{-1}$ ; the velocity of the star itself is near  $-16 \text{ km s}^{-1}$ . A number of these complex shell lines have been decomposed in the following way. Each component was represented as a pure absorption line of depth  $e^{-\tau}$ , where  $\tau$  was gaussian (of the form  $\exp(-0.5(\delta v/\sigma)^2)$ ) whose velocity, depth, and FWHM could be adjusted; the observed profile followed by adding the individual  $\tau$ 's at every pixel across the line. Figure 6 shows fits to Ti I  $\lambda 4999$ , where dashed lines outline the individual components, the solid line the observed profile, and a series of crosses show the representation. Table 2 gives the parameters found to fit 2 representative T I lines as well as Ba II  $\lambda 6496$ , Li I  $\lambda 6707$ , and Rb I  $\lambda\lambda 7800, 7947$ .

A source of uncertainty in these fits was the choice of continuum level under the shell line. Ideally that would be the underlying photospheric line spectrum as represented by an artificially broadened F-G supergiant (as in Fig. 5), but it was clear that an adequate match could be achieved only by adding in a veiling continuum as well. Until this effect could be understood, and applied in a consistent wavelength-dependent fashion, it was decided simply to interpolate the continuum level linearly between two points just outside either edge of the shell line. The equivalent widths of components 1 and 2 are particularly susceptible to errors in the continuum level so defined.

Nine unblended Ti I lines having lower levels between 0.0 and 1.4 eV were synthesized in this way. For each of the 5 shell components, the EWs were fitted to a theoretical pure-absorption curve of growth, and the values of the parameter  $\xi_0$  (the Doppler width in velocity units), the excitation temperature  $T_{\text{exc}}$  and the total Ti I column density  $N(\text{Ti I})$  extracted. They are listed in Table 3. These temperatures are estimated to be uncertain by several hundred degrees. For most components  $\xi_0$  ranges between about 2 and 5  $\text{km s}^{-1}$ , inter-

mediate between the thermal velocities for Ti (1.1 km s<sup>-1</sup>) and H (8 km s<sup>-1</sup>) at the  $T_{exc}$ 's of Table 3. However the measured FWHMs of the individual Ti I shell lines scatter between about 8 and 19 km s<sup>-1</sup> (following allowance for the instrumental FWHM of 6 km s<sup>-1</sup>). This shows that there is another source of line broadening in these expanding shells, possibly weak unresolved structure.

Eight unblended Fe I shell lines were analyzed in the same way. The scatter in the fit of the gaussian EWs to the curve of growth was much larger than for Ti I, possibly because of greater uncertainties in defining the continuum level. Only the results for the -78 and -61 km s<sup>-1</sup> components are considered reliable. The  $T_{exc}$  for Fe I was very clearly lower than for Ti I, between about 1350 and 1500 K. The total column density if  $T_{exc} = 1500$  K is near  $\log(N(Fe\ I)) = 17.4$ . This difference between the  $T_{exc}$ 's of Ti I and Fe I is puzzling, because their identical velocity structures indicate that they originate in the same parcels of rising gas. Possibly non-LTE conditions in the shell are responsible.

The evolution of the shell and wind absorptions during the brightness minimum of 1996–2001 is shown in Figure 7, from SOFIN spectra. One might expect that the shell features would be stronger at minimum brightness, but in fact at minimum in 1998–1999 it was the *wind* features that were enhanced, while the shell components were strongest in 1996–97 and 2001. This is illustrated in Figure 8, which compares the 4660–4690 Å region on the HIRES spectrogram of 1997 Aug. 12 (below) with that of 1998 Oct. 30 (above). The Ti I shell lines (4667.58 and 4681.91 Å) were strong on the first date but had essentially disappeared 15 months later. At that second date, weak, narrow emission lines (arrowed) at approximately the stellar velocity were detectable.

An unusual feature of the shell spectrum is the prominence of the lines of Rb I at 7800 and 7947 Å. Their EWs in the -78 km s<sup>-1</sup> component were 194 and 127 mÅ in 1997 August. The first ionization potential (IP) of Rb is 4.8 eV, so one would expect it to be ionized because barium, with first IP = 5.2 eV and a comparable meteoritic abundance to rubidium, is detectable only as Ba II ( $\lambda 6496$ , EW = 267 mÅ). The non-detection of Cs I  $\lambda 8521$  is understandable because of the still lower first IP of cesium (3.9 eV) and a lower meteoritic abundance

(Rb/Cs = 19), but the strength of Rb I remains unexplained.

## 2.4. The Emission Lines

Before 1997, the only obvious optical emission lines in V1057 Cyg were the components of the P Cyg structure of H $\alpha$  and Ca II. In that year, when the star had begun its decline following the 1985–1994 plateau, a number of emission lines of low excitation appeared in the centers of the corresponding stellar absorptions (Petrov et al. 1998). The most conspicuous were Fe I [RMT 12] 8047 and 8074 Å, followed by Fe I [60] 8514, Fe II [40] 6516, Ca I [1] 6572, and Fe I [12] 7912 Å: Figure 9. These emission peaks are at about the stellar velocity, and are narrower than the photospheric absorption lines. A higher-resolution HIRES spectrogram of 1997 August 13 confirms the asymmetry of the  $\lambda\lambda$  8047, 8074 lines that is apparent in Figure 9: their shortward edges are clearly steeper than the longward. Most of these same low-excitation emission lines were observed long ago in the G supergiant  $\rho$  Cas by Sargent (1961).

This appearance of emission in the centers of many low-excitation absorption lines is illustrated in Figure 10 which compares the 6400 Å region on a Lick coudé spectrogram of 1985 May 27 (resolution about 18 km s<sup>-1</sup>) with the HIRES spectrogram of 1997 Aug. 13, slightly smoothed. In those intervening 12 years, the centers of the Fe I absorption lines  $\lambda\lambda$  6393, 6400 increased in brightness with respect to the continuum, rising at peak to almost the continuum level. (A second Lick spectrogram obtained on 1985 Sept. 25 showed no change had taken place during those 4 months.)

We believe that this emission spectrum is produced in a warm layer we call a ‘chromosphere’ that is almost overwhelmed by the photospheric continuum when the star is bright, except through its marginal appearance as emission cores in lower-excitation stellar absorption lines. However, that chromosphere must have become brighter by a factor of about 2 between 1985 and 1997. The reason: between those dates V1057 Cyg faded by only about 0.9 mag. in V, so if the 1997 emission cores in  $\lambda\lambda$  6393, 6400 had been present at that same absolute brightness in 1985, they would have filled those absorption lines up to about half the depth actually observed.

To determine whether there was any further change in the brightness level of the chromosphere, the EWs of several emission cores were measured in the SOFIN differential spectra (§ 2.5) of V1057 Cyg (minus  $\beta$  Aqr spun up to  $v_{\text{eq}} \sin i = 55 \text{ km s}^{-1}$  and not veiled) between 1996 and 2001. The results are given in Table 4. Over these years, the emission line EWs remained constant within the errors of measurement; i.e. as the star faded, the lines became weaker in the same proportion. We conclude that there was no further change in the absolute intensity of the chromosphere after the increase by a factor of approximately 2 sometime between 1985 and 1997.

This brightening of the chromosphere may have been related to the increase in the wind activity that began in 1984-85 (§ 2.2).

As V1057 Cyg has declined in brightness, the fading of the continuum has helped to reveal this chromospheric emission spectrum. We believe that it is this spectrum that is responsible for the apparent ‘doubling’ of some absorption lines that has been suggested as evidence of orbital motion in a Keplerian disk. In an earlier paper on the spectrum of FU Ori (Petrov & Herbig 1992) we argued for such an explanation of the ‘doubling’, a possibility in fact first mentioned by Goodrich (1987). The fading of V1057 Cyg has now provided strong support for that interpretation.

These central reversals which have emerged as distinct emission lines since 1995 are not very strong, e.g., Fe I  $\lambda 8047$  has a peak intensity of only 5–8% above the continuum level. If the continuum were one magnitude brighter (or the chromosphere fainter), the line would appear only as an emission core at the bottom of a broader photospheric absorption, as in Li I 6707 Å (Fig. 9). For a quantitative analysis of this emission spectrum, the underlying photospheric contribution must first be subtracted. This is described below (§ 2.5), as is a comparison with the low-temperature ( $T_{\text{exc}}$  about 2700 K) emission spectrum of VY Tau at the time of a flare-up, to which it bears a strong resemblance.

The central intensities of such chromospheric emissions would, in the optically thick limit, rise to the Planck flux at that temperature. Therefore—depending in individual cases upon  $gf$  value and lower EP—the strengths of those lines with respect to the hotter photospheric continuum would tend

to increase toward longer wavelengths. This would explain the greater prominence of line ‘doubling’ in the red than at shorter wavelengths that has been noted, for example, by HK.

The strong Ca II H & K emission lines at 3933, 3968 Å (discussed in § 4.5) and at the infrared triplet are probably produced in this chromosphere, presumably the same that D’Angelo et al. (2002a,b) found necessary to reproduce the H $\alpha$  profile of FU Ori. The Balmer emission lines that ought to be produced in the same region are concealed by the P Cyg structure of the wind, except for the longward emission fringe at H $\alpha$ . The shortward edges of the Ca II emission lines are truncated by their own P Cyg absorptions. Clearly, the outflowing wind is located *above* this chromosphere, demonstrated also by the presence of fluorescent Fe I 4063 and 4132 Å lines in V1057 Cyg: those Fe I atoms “see” the exciting Ca II  $\lambda 3968$  emission line, although it is hidden from us by the wind component of H $\epsilon$ .

A very broad emission, at peak only about 0.12 above continuum level, is present at 6297 Å on the HIRES spectrum of 1997 August 13 (that region falls between orders on other exposures). It must be [O I]  $\lambda 6300.30$  because the weaker [O I] line at 6363 Å is present on other HIRES and SOFIN spectra of 1996–1998. The central velocity of  $\lambda 6300$  is about  $-135 \text{ km s}^{-1}$ , its total width at continuum level about  $180 \text{ km s}^{-1}$ . A similar broad, shortward-displaced emission line is also present at the position of [Fe II]  $\lambda 7155$ . They have nearly the same velocity as the “intermediate case between shell and wind” components mentioned in § 2.3. No such features are found in FU Ori.

The reader should be aware that FUors are not unique in possessing broad absorption lines with emission cores and CO absorption in the  $2 \mu\text{m}$  region: a number of normal (i.e. not pre-main sequence) F- and G-type high luminosity stars are known to have such spectra. Several examples were mentioned by Petrov & Herbig (1992) and more recently, the classical case of  $\rho$  Cas has been rediscussed by Lobel et al. (1998).

To summarize, in addition to the photospheric spectrum, these sets of spectral features were present in V1057 Cyg during this period at different radial velocities:

wind at  $-100$  to  $-300 \text{ km s}^{-1}$  (H $\alpha$ , D<sub>12</sub> Na I,

Ca II, Mg I, Fe II);

shell at  $-40$  to  $-110$  km s $^{-1}$  (TiO and low excitation atomic lines in absorption);

CO molecules at about the stellar velocity (§ 3.5); and

low-excitation chromospheric emission at the stellar velocity.

## 2.5. The Differential Spectrum

As already pointed out, a number of low excitation lines clearly went into emission above the continuum during the brightness minimum of 1996–2001. It is natural that the same feature should be present in higher excitation lines if only as an emission core at the bottom of the absorption line, but enough to cause those lines to appear double and shallow, as is observed (Petrov & Herbig 1992; Petrov et al. 1998). Such line emission can be revealed by subtracting the underlying photospheric spectrum. As a template for the photospheric spectrum of V1057 Cyg we use  $\beta$  Aqr spun up to  $v_{\text{eq}} \sin i = 55$  km s $^{-1}$  and veiled by a factor 0.3. Two fragments of this differential spectrum are shown in Figure 11 for the average spectrum of 1998–2000. Note that the relative strength of the emission lines is not the same as in the absorption spectrum.

Both the “true” emissions (that rise above the continuum) and those revealed in such a differential spectrum fall along a common curve of growth for  $T_{\text{exc}} = 3600 \pm 300$  K,  $\log n_e = 7.5 \pm 0.5$ . This temperature is significantly lower than photospheric. In the M-type dwarf VY Tau, the same emission lines appeared very strong by contrast with that low temperature continuum Herbig (1990). There is a good correlation between the equivalent widths of the low-temperature line emissions in VY Tau and those in the differential spectrum of V1057 Cyg; Figure 12.

The same method was used by Welty et al. (1992) to reveal the emission lines in the differential spectra of FUors, but the template they used for subtraction was the accretion disk model spectrum. The line depths in V1057 Cyg are now very different from both  $\beta$  Aqr and that disk model (Fig. 13).

Although the observed line intensities can be explained as a sum of the photospheric and emis-

sion line spectra, the observed *line profile* is not just a sum of two gaussians. Weaker lines have a rather “boxy” shape, with sharp edges, while stronger lines (without shell components) have nearly normal rotational profiles except for the emission cores. This difference suggests some abnormality in the structure of the lower atmosphere, deserving of attention at high resolution  $\geq 60,000$  and S/N  $\geq 300$ .

## 3. V1057 Cyg: Interpretation of the Light Curve

Conventional assumption is that a FUor outburst represents only a temporary event and that the star will eventually return to its former brightness. The slow fading of FU Ori over the past 60 years, and the relatively rapid decline of V1057 Cyg since about 1971 might be explained in this way. But the spectrum of V1057 Cyg does not support this expectation. Before the 1970 outburst, the star possessed H $\alpha$  emission that, in order to have been detected at all in the first low-resolution surveys, by Haro (1971) in the early 1950s and by Herbig (1958) in 1952–56, must have had an equivalent width of approximately 25–40 Å. No such emission has appeared at H $\alpha$  during the decline to the 1999–2000 minimum: the emission fringe has remained near  $\text{EW}(\text{H}\alpha) = 1\text{--}2$  Å (Table 1).

Another departure from expectation is the following. Before the outburst a number of Fe I and Fe II emission lines were reported Herbig (1958), so they must have been fairly strong to have been detectable on that 1957 low-dispersion photographic spectrogram. Yet at the present time no Fe II emission lines are detectable in the blue-violet on modern, far superior digital spectrograms, although the fluorescent Fe I 4063, 4132 Å lines are weakly present.

Furthermore, as the star has declined one would have expected the absorption spectrum to approach that of a TTS-like K- or M-type dwarf. In 1998–1999 V1057 Cyg was only about 1.5 mag. (in B) above its pre-outburst level (B = 14.9) so if the star was returning to its original T Tau state, a late type photosphere and emission line spectrum ought to have emerged. But in spite of the drop in brightness, the spectral type of V1057 Cyg remained the same as in the 1980’s: in § 2.1 it was shown that the star continues to resemble a

rapidly rotating G supergiant, unlike any other pre-main sequence star of which we are aware. But the spectroscopic similarity is deceptive: the  $M_V$ 's are quite different. If the surface brightness and  $(V-R)_J$  color of V1057 Cyg at the time of the 1985–1994 plateau were the same as those of the standard G0 Ib  $\beta$  Aqr, then correction for  $A_V = 2.35$  mag. leads to  $M_V = +0.3$  for a distance of 600 pc.<sup>5</sup> This compares to  $M_V = -3.5$  for  $\beta$  Aqr. That  $M_V$  for V1057 Cyg would be produced by a single star of uniform surface brightness having a radius of about  $9 R_\odot$ .

Given these considerations, and the fact that V1057 Cyg both pre- and post-outburst was unusual in its possession of a very massive high-velocity wind (§ 4.5), we later speculate that pre-outburst FUors are not normal TTS, but represent a special sub-species of that class.

We suggest that the behavior of V1057 Cyg as it has faded, as well as for the general spectroscopic properties of the classical FUors, may be understood in terms of a stratified atmosphere atop a rapid rotator with a strong quasi-permanent outflowing wind, a low effective  $g$  being responsible for the line-spectrum resemblance. The emission spectrum which has appeared as the continuum of V1057 Cyg has faded is, as we have stressed, that of a low-excitation chromosphere atop the stellar atmosphere (§ 2.4).

The decline of V1057 Cyg from its 1971 peak brightness to the plateau level in 1985–94 can be represented by a continuous change in radius and surface brightness of a rapid rotator, those quantities being derivable from the procedure of Barnes et al. (1976) and the above values of extinction and distance. Observed  $V$  and  $(V-R)_J$  for 1971–2001 were taken from Kopatskaya et al. (2002), for 1978–2001 from Ibrahimov (1996, 1999, and private communication), and for 1971 from Mendoza (1972) and Rieke, Lee, & Coyne (1972). The resulting values of  $R/R_\odot$  are plotted in Figure 14. The symbols identifying the sources of the photometry are explained in the caption.<sup>6</sup> Radii and

<sup>5</sup>This distance is based on the colors of stars in the general vicinity of NGC 7000 (Herbig 1958; Laugalys & Straizys 2002).

<sup>6</sup>Kopatskaya (1984) also used the Barnes, Evans, & Parsons formulation to calculate  $R/R_\odot$ , but from its dependence on  $B-V$ . Our radii come instead from the dependence on  $(V-R)_J$ , following the recommendation of Barnes et al.,

surface brightnesses depend upon whose colors are used. If the Ibrahimov data, Figure 14 shows how  $R/R_\odot$  fell from about 14 near maximum light to about 9 at the time of the plateau. The surface brightnesses declined from values appropriate a late A-type main sequence star in 1971, to a mid-K type in 1995.

We emphasize that such calculations *do not prove* that the source is a spherical star, only that the brightness and color can be represented by a circular surface of those dimensions and surface brightness.

In 1984–85 the wind flux began to increase (§ 2.2), and at about the same time the decline in brightness halted. Sometime between 1985 and 1997—we speculate that it may have been early in that interval—the chromosphere is known to have brightened with respect to the continuum. Thus all three phenomena may have been consequences of an upsurge of activity in the underlying rapidly rotating star.

The plateau episode ended when, between 1994 and 1995, the star abruptly became fainter by 0.78 mag. in  $B$ , and redder by 0.18 mag. in  $B-V$  (seasonal averages); see the small plot of  $B-V$  vs time at the bottom of Figure 1. The ratio  $\Delta B/\Delta(B-V) = 4.3$  is not far from the standard interstellar reddening value (4.1). Thereafter (§ 2.4) the continuum and chromosphere fluctuated in brightness together, so we ascribe the 1994–95 fading to screening by a dust layer somewhere higher in the atmosphere. This is not a new idea: the possibility of dust condensation in the outflowing wind of V1057 Cyg has already been raised by Kolotilov & Kenyon (1997), and it will be recalled that Kenyon et al. (1991) interpreted a relatively brief dimming of the FUor V1515 Cyg in 1980 as such an event. The formation of such a dust layer was also envisioned by Rao et al. (1999) in the case of R CrB, also a high-luminosity G star.

However V1057 Cyg continued to fade,  $\Delta B = 0.63$  mag. by 1999, apparently without any further change in color. Either more dust dominated by large particles, or a continuation of the slow post-1971 decline, could be responsible.

and the fact that an excess shortward of 4800 Å was present between 1971 and 1975–76 (Herbig 1977, Fig. 8), which would make  $B-V$  suspect. It is of course unclear which color is more likely to be applicable to an unusual object like V1057 Cyg.

The foregoing is an attempt to pull together the photometric and spectroscopic phenomena exhibited by V1057 Cyg since the 1970–71 outburst. However, it is likely that the atmospheric structure is not radially homogeneous, as this picture may seem to imply. The day-to-day and secular fluctuations observed in the H $\alpha$  structure at both V1057 Cyg and FU Ori show that wind ejection is spasmodic, possibly coming from localized areas on the rotating star, rather as the fast solar wind emerges from ‘coronal holes’ on the Sun. It would then not be surprising if the wind fields above these stars contained much structure. The HST images of V1057 Cyg (§ 3.1) show that the distribution of dust near that star, whether formed in and ejected by the star or local dust shaped by the stellar wind, is highly structured.

The disappearance and reappearance of the shell spectrum of V1057 Cyg on a time scale of a few years cannot be due to pure radial expansion and the consequent decline in column density proportional to  $r^{-2}$ . It may be caused by the movement of inhomogeneities in the wind structure across the line of sight. The broad shortward-shifted [O I] and [Fe II] lines described in § 2.4 could then arise in this expanding, inhomogeneous envelope, their longward wings being occulted by the star.

Unexplained is the veiling mentioned earlier that was used to account for the general shallowing of the absorption spectrum. It is conceivable that the line shallowness is intrinsic, i.e., the result of integration over a very non-uniform stellar hemisphere, or of line formation in a highly non-spherical extended atmosphere, or of the contribution of a continuum originating in the chromosphere. If extrinsic, thermal emission by dust is an unlikely explanation, because although the energy absorbed in the hypothetical dust layer must reappear somewhere, dust would not survive at temperatures greater than about 1500 K so that that re-emission would be significant only at long wavelengths, not in the optical.

### 3.1. Direct Images of V1057 Cyg

If dust did form in the lower atmosphere of V1057 Cyg in 1994 and was subsequently expelled with the wind, then in time it might become detectable in scattered light. Given an ejection velocity of 200 km s $^{-1}$  and no subsequent deceleration

then the separation of dust and star in the plane of the sky would increase at the rate of 0''.07 yr $^{-1}$ , so that in the 5 years following 1994 that dust would in projection appear about 0''.35 from the star.

Five WFPC2 images of V1057 Cyg are available in the HST archive. They were obtained with HST on 1999 Oct. 18 as part of a ‘snapshot’ program; the filters were F606W (central wavelength 5957 Å) and F814W (7940 Å). We are grateful to Karl Stapelfeldt, the Principal Investigator, for the opportunity to study this material. We did no more than obtain the pipeline processed images from the Archive and trim and clean up cosmic ray hits and other defects.

Those F606W images are shown in Figure 15. There is much scattered light and spurious structure surrounding the overexposed star image, so that nothing can be said whether structure exists as near as 0''.3 from the star. However, at least three features at somewhat larger separations are present and appear to be real, judging from inspection of similar images of ordinary stars on other WFPC2 frames taken in the same series. They are identified by letters. C is the brightest; it appears as a structureless blob protruding from the star image to a distance of about 1'', while A and B are fainter, curved arcs reminiscent of the larger loops at V1057 Cyg and other FUors described by Goodrich (1987). The arc D is more distant, and is located at the base of a similar structure present on ground-based images of V1057 Cyg obtained in the 1970s (Duncan, Harlan, & Herbig 1981). The reality of A, B and C is confirmed when the image of a single star (from another frame) is subtracted from the shortest F606W exposure: see the lower right panel of Figure 15. The feature C is apparently only a section of an extended nebulous bar. There is no persuasive correspondence of this structure very near the star with the molecular-line or 1.3 mm continuum maps of McMuldron (1995).

If C is a slab of warm dust very near the star, consider the possibility that its thermal emission may contribute significantly to the integrated IR emission of V1057 Cyg. An estimate of its relative contribution can be made as follows. Assume that the true separation of star and slab is as projected, 0''.8 (480 AU), and that the star radiates as a black body of  $T_{\text{eff}} = 5300$  K and radius  $9 R_{\odot}$ . Then the

equilibrium temperature of a small silicate particle exposed to that radiation field is obtained by balancing the energy absorbed by the amount re-radiated. Given the absorption cross-sections for ‘astronomical silicate’ (Draine 1985), the temperature of a  $0.1\text{ }\mu\text{m}$  silicate particle at that position is found to be about 75 K, with a weak dependence on particle radius. If the slab, an assemblage of such particles, radiates as a black surface of dimensions  $0''.33 \times 0''.64$  at 75 K, then its flux would be dominant over that of the star at wavelengths greater than about  $14\text{ }\mu\text{m}$ . On the other hand, if the slab preserved the optical properties of its constituents, then the crossover wavelength would depend on particle radius, being at about  $19\text{ }\mu\text{m}$  for  $0.1\text{ }\mu\text{m}$  particles, at  $16.5\text{ }\mu\text{m}$  for  $0.4\text{ }\mu\text{m}$ , and at  $15.5\text{ }\mu\text{m}$  for  $1.0\text{ }\mu\text{m}$ . Obviously, thermal emission from such nearby dust must contribute to the SED’s of stars like V1057 Cyg, although to lesser degree than these estimates if the cloud were optically thin.

Dust formed in the atmosphere of V1057 Cyg and then ejected could have reached the slab’s present position in as short as 12 years. Nothing is known of the earlier history of V1057 Cyg but if there have been previous outbursts, each with its own dust-formation episode, such distant dust concentrations might be explained. Future high-resolution imaging will show whether these structures are moving with respect to V1057 Cyg.

Unfortunately no comparable HST imagery is available at this time for FU Ori. Conventional ground-based CCD images obtained with the 2.3-m telescope on Mauna Kea show extensive reflection nebulosity around that star, with brightness increasing toward the star before merging at about  $3''$  with the overexposed star image. Coronagraphic images reproduced by Nakajima & Golimowski (1995) extend this in to about  $2''.5$ . As at V1057 Cyg, this material and that detected at  $2.3\text{ }\mu\text{m}$  very near FU Ori by Malbet et al. (1998) may contribute significantly to those SED’s.

#### 4. FU Ori, V1057 Cyg and FUors in General

##### 4.1. Comparison with the Composite Spectrum of an Accretion Disk

Accretion disk models were devised by Kenyon et al. (1988) to explain the spectral energy dis-

tribution and the peculiar double-peak profiles of the photospheric lines in V1057 Cyg and FU Ori. In those models, the high-resolution spectra were synthesized by assuming that at any given radius the disk radiates as a stellar atmosphere of the appropriate spectral type. The variation of effective temperature with radius is given by the steady disk theory, and the variation of the rotational velocity with radius is assumed to be Keplerian. The integrated spectrum of the disk can then be represented as a composite of annuli of different temperature, surface brightness, and rotational velocity. The models reproduce reasonably well the atomic lines in the optical region and the molecular bands in the infrared. In addition to FU Ori and V1057 Cyg, the spectrum of Z CMa was compared to the disk model by Welty et al. (1992), revealing numerous emission lines in the differential spectrum (i.e., observed minus synthetic) of Z CMa, rather as is seen in V1057 Cyg near minimum brightness.

However not all spectral lines can be reproduced by the disk model. Some lines in regions of the spectrum not examined by Kenyon et al. are in striking contradiction to the model prediction. Because the spectrum of V1057 Cyg has changed due to the increasing prominence of line emission as the star has faded toward minimum brightness, in what follows we first demonstrate these discrepancies in the spectrum of FU Ori because it has not changed significantly over the last two decades.

New synthetic disk spectra were calculated for FU Ori and V1057 Cyg using the parameters of the disk models given by Kenyon et al. (1988) and a set of our own template spectra (see Table 5) obtained at the Nordic Optical Telescope with SOFIN. As an example, the synthetic and the observed spectra of FU Ori are shown in Figure 16 for the spectral range 5260-5320 Å. This synthetic spectrum looks identical to that shown in Figure 3 of Welty et al. (1992). The spectrum of FU Ori in 1998 was also very similar to that displayed by Welty et al..

In the accretion disk model for FU Ori, the relative contribution from different parts of the disk (i.e., from different spectral types) to the total flux radiated by the disk depends on wavelength as is shown in Table 6 [contribution]. At 5500 Å the spectrum of the disk is mostly of F-G type, while at 9000 Å all spectral types contribute about equally. This means that at 9000 Å one can find

F-type spectral features along with M-type, e.g., both high-excitation lines and TiO bands.

If we consider relative line strengths, the composite spectrum of the accretion disk looks much the same as the spectrum of a normal G supergiant because the same atomic lines are changing smoothly from late F through G to early K types. The difference can be found only in early type F, where the lines of high-excitation species appear strongly, and in type M where molecular bands, mostly of TiO, appear very strong. Since both F and M spectral types contribute to the accretion disk model of FU Ori, we examine the observed spectrum in order to determine how these critical features behave.

The most suitable spectral region for such an analysis is around 8900 Å. It contains two Ca II lines having lower EP of 7.05 eV (8912.06 and 8927.35 Å) which are very strong only in type F, a line of V I at 8919.80 Å having EP = 1.2 eV which increases in strength from type G to M, and a strong TiO bandhead at 8860 Å, characteristic of type M.

The telluric spectrum was extracted from a spectrum of the O7e fast rotator  $\xi$  Per, and with it weak terrestrial lines were removed from the FUor spectra. In order to reduce the noise, all the spectra of FU Ori taken in 1997–2000 were averaged. For V1057 Cyg, to avoid a possible contribution from the shell, only the 1998–2000 spectra were averaged because in those years the shortward-shifted TiO features were absent.

Comparison of the synthetic spectrum of the accretion disk and the observed spectrum of FU Ori is shown in Figure 17. Some of the template spectra are also displayed in the Figure to show the origin of the main features in the synthetic spectrum. As expected, the synthetic spectrum of the accretion disk shows all the F- and M-type features. In the observed spectrum of FU Ori the blend at 8860 Å resembles that in the synthetic spectrum, except that the TiO head is not obviously present probably on account of the overlap by Paschen line at 8862 Å. The absence of TiO is better shown in V1057 Cyg (Fig. 21, below). More obvious is the difference between the observed and synthetic spectra in the width of the Ca II and V I lines. That region is expanded in Figure 18. In the synthetic spectrum these lines have very different widths because they originate from the

innermost and from the outermost regions of the disk, respectively rotating at very different Keplerian velocities, but in the observed spectrum the lines have about the same widths.

Another example is shown in Figure 19: the high-excitation line of N I  $\lambda$ 7442.30, EP = 10.3 eV, is strong in the F-type spectra, is present and highly doubled in the synthetic spectrum of FU Ori but is absent in the observed one. Figure 20 shows that the ScO/TiO feature at 6036 Å is absent in the observed spectrum of FU Ori, while it is quite obvious in the synthetic.

The 8900 Å spectral region in V1057 Cyg also reveals a difference between observed and model spectra (Fig. 21). Since the rotational velocity is lower than in FU Ori, the TiO head is well resolved in the model spectrum. The TiO feature is clearly absent in the average spectrum of V1057 Cyg, or in the noisier 1998–2000 individual spectra.

Here we have considered only those spectral features detectable at the resolution of the SOFIN material. Much more could be done with spectra of higher resolution. But at the moment we conclude that comparison of the observed and synthetic spectra of FU Ori in the near infrared shows that some critical spectral features do not have the structure predicted by the multi-temperature disk model, although some elaboration of that model might be able to account for the mismatches. A rapidly rotating single star will have a latitude-dependent spectrum, whose appearance in integrated light will be a function of aspect angle. It remains to be seen if such an object might produce a FUor-like spectrum.

## 4.2. Rotational Line Widths

The value of  $v_{\text{eq}} \sin i$  and the nature of the photospheric line broadening in FUors have been a subject of much discussion. Welty et al. (1990, 1992) measured absorption line widths on V1057 Cyg spectrograms obtained in 1986 and 1988 when the star was brighter, and found them to depend on wavelength, being larger in the blue and smaller in the red. This they interpreted as demonstration of differential rotation in a Keplerian accretion disk, as predicted by the HK disk model.

The shortward-displaced shell spectrum had been present at some level on all our spectra of V1057 Cyg, but is most prominent at the shorter

wavelengths where most of the low-level lines of the neutral metals are located. It was very strong in 1996–97, so  $v_{\text{eq}} \sin i$  was measured only on the 1998–2000 SOFIN spectra and as an additional precaution, to avoid any marginal shell contribution, only the longward wings of the photospheric lines were fitted. Thirty selected lines were compared to the template spectrum ( $\beta$  Aqr, G0 Ib) spun up to a set of discrete values of  $v_{\text{eq}} \sin i$ . Since the line depth in V1057 Cyg at that time was smaller than in the template, a veiling contribution (which does not affect the line width) was applied to rescale the line depth.

The result was that in V1057 Cyg the average  $v_{\text{eq}} \sin i = 55 \text{ km s}^{-1}$ , with a scatter of individual lines mostly between 50 and 60  $\text{km s}^{-1}$ . No systematic trend with wavelength was present in the range 5000–9000 Å, nor was there any trend with EP in the range 1–8 eV. The minimal level of veiling is about 0.3. It is larger for individual lines filled in with emission, especially those of lower EP (see below).

This value of  $v_{\text{eq}} \sin i$  (55  $\text{km s}^{-1}$ ) is larger than those published by Welty et al. (1990) (35–45  $\text{km s}^{-1}$ ). However, they measured line half-widths at half depth, which in a rotationally broadened profile is about 0.8  $v_{\text{eq}} \sin i$  (the precise value of the factor depending slightly upon the limb darkening assumed). We have also measured the half-widths of the red wings at half depth: the average value is  $44 \pm 4 \text{ km s}^{-1}$ , in agreement with Welty et al., but again we found no dependence on wavelength or EP. It is possible, of course, that the spectrum of V1057 Cyg changed in this respect during the intervening decade.

The same procedure described above (fit of longward wings to the spun-up template) was carried out for FU Ori. The best fit was with  $v_{\text{eq}} \sin i = 70 \text{ km s}^{-1}$ , and again no relationship between  $v_{\text{eq}} \sin i$  and EP or wavelength was found. It would not seem likely that the spectrum of FU Ori has changed significantly since the Welty et al. observations.

### 4.3. CO Lines

On 1999 Oct. 24 both V1057 Cyg and FU Ori were observed in the 2.3  $\mu\text{m}$  region by K. Hinkle with the Phoenix infrared spectrometer (Hin-

kle et al. 1998) at the KPNO<sup>7</sup> 2.1 m telescope. The region covered was 4320 to 4340  $\text{cm}^{-1}$  (2.315 to 2.304  $\mu\text{m}$ ) in the 2-0 CO band. These spectrograms had been obtained at the request of Lee Hartmann, and we are grateful to him for access to the data and to Ken Hinkle for supplying us with the reduced spectra, as well as those of several early-type stars observed on the same occasion.

This region contains many terrestrial lines, mainly of  $\text{CH}_4$ . These are not removed completely by standard star division because of airmass mismatches. Instead, the value of optical thickness (required to reproduce the line depth as  $\exp(-\tau)$ ) was calculated at every pixel across these features in the standards, which was then scaled to cancel those features in the FUor spectra. These spectra of FU Ori and V1057 Cyg are shown in the upper rows of Figure 22. The dominant features are the broad R-branch lines of the CO 2-0 band (R(19) through R(27): lower EP 0.09 to 0.18 eV). Their equivalent widths are comparable to those of early to middle-M type giants and supergiants in the atlas of Wallace & Hinkle (1996), from which the FTS spectrum of  $\lambda$  Dra (type M0 III) in the bottom section of Figure 22 has been extracted. The same spectrum spun up to  $v_{\text{eq}} \sin i = 60 \text{ km s}^{-1}$  is shown just above. In  $\lambda$  Dra the lines of the returning R-branch (R(75) through R(81): lower EP 1.33 to 1.55 eV) are strong, but they are not apparent in either FUor. Although they would be masked to some degree by the greater line widths, the lack of convincing and consistent asymmetries in the FUor lines due to these blends suggest a lower rotational temperature.

The CO lines have different shapes in the two FUors: in FU Ori they are broad and essentially symmetric, while in V1057 Cyg they are asymmetric, with a narrow core and an extended wing toward negative velocities. To reduce the effects of instrumental noise and that introduced by atmospheric line removal, the line profiles shown in Figure 23 were created by averaging the 4–5 least noisy CO lines for each star. These were fitted by a procedure similar to that described in § 2.3. The instrumental profile, represented by that of a narrow atmospheric  $\text{CH}_4$  line of  $\text{FWHM} = 8 \text{ km s}^{-1}$ ,

<sup>7</sup>KPNO is operated by the Association of Universities for Research in Astronomy, Inc. under cooperative agreement with the National Science Foundation.

could be spun up to adjustable  $v_{\text{eq}} \sin i$ , central velocity, and central depth. The parameters of the fits are given in Table 7. Although the off-center structure in FU Ori may be real, a single component serves to represent the overall profile reasonably well. In the case of V1057 Cyg, the observed profile is certainly *not* a narrower version of the stellar absorption lines. Formally, it can be fitted to two overlapping, rotationally broadened copies of the atmospheric line. Because of the complex structure, comparison of these  $v_{\text{eq}} \sin i$ 's with the optical value cannot be very meaningful.

In neither star is there any evidence of shell structure at large negative velocities, perhaps understandably because the shell spectrum in the optical was very weak at the time of the CO observation. The CO velocity of FU Ori agrees closely with the conventional velocity of that star ( $+28 \text{ km s}^{-1}$ ), in agreement with Mould et al. (1978), who found “from several CO and metal lines” a value of  $+28.2 \pm 2.5 \text{ km s}^{-1}$ . However, the velocities of both CO components of V1057 Cyg (Table 7) are displaced from the optical  $-16 \text{ km s}^{-1}$ , nor do they agree with the Mould et al. value of  $-13.4 \pm 3.5 \text{ km s}^{-1}$ .

In the case of FU Ori, the value of  $v_{\text{eq}} \sin i$  from CO ( $48 \text{ km s}^{-1}$ ) is clearly smaller than that we obtain from the optical region ( $70 \text{ km s}^{-1}$ ), in the same sense as earlier work by the CfA group. Hartmann & Kenyon (1987a) measured total widths of cross-correlation peaks rather than  $v_{\text{eq}} \sin i$ 's, so the two results cannot be compared directly, except to say that they found the CO lines in FU Ori to be narrower than the optical by a factor of about 0.75, as compared to our 0.69. In V1057 Cyg also, the stronger CO component ( $45 \text{ km s}^{-1}$ ) is narrower than the optical total  $v_{\text{eq}} \sin i$  of  $55 \text{ km s}^{-1}$ , but this may not be significant because the CO profiles are peculiar. The only published CfA result for CO in V1057 Cyg is an estimate that  $v_{\text{eq}} \sin i$  is about  $20 \text{ km s}^{-1}$  (Hartmann & Kenyon 1987b).

#### 4.4. Search for Rotational Modulation in Line Profiles

In T Tauri stars (TTS), a period of axial rotation can be derived from rotational modulations of brightness and line profiles caused by surface inhomogeneities (cool or hot spots) and nonaxisymmetric structure of the wind (see, e.g., Petrov et

al. 2001). Unlike an ordinary star, an accretion disk has no single rotational period but a range of Keplerian orbital periods. In the accretion disk models for FU Ori and V1057 Cyg (Kenyon et al. 1988), the Keplerian periods range from 3–4 days for the inner disk where the F-type spectrum is formed, to 30–40 days for the outer regions contributing to the M-type spectrum. Thus an observational test would be to search for rotational modulation in the wind, emission and photospheric line profiles. The most prominent wind feature is the H $\alpha$  P Cyg line. The emission lines of metals are present only in the spectrum of V1057 Cyg and are too weak to be used in such an analysis because the individual spectra of V1057 Cyg near minimum brightness are rather noisy. The photospheric lines, although also being weak, can however be analyzed by cross-correlation, which compensates for the poor signal-to-noise ratio of the individual spectra.

##### 4.4.1. Wind Profiles

Figures 24 and 25 show overplotted all the H $\alpha$  profiles from the SOFIN data of 1995–2001 for V1057 Cyg and FU Ori, the latter in two parts to emphasize the major changes in the longward emission component. The left panel is a superposition of all the profiles of FU Ori in which the emission peak intensity was greater than 1.20 (in continuum units), and the right panel all those with peak less than 1.10. As already mentioned, there is no obvious correlation between these emission peak intensities and the extension of the P Cyg absorption component to negative velocities.

The time scale of the variability is different in the two objects. In V1057 Cyg, the night-to-night variability is relatively small, but the average profile is quite different in different years (see also Fig. 7). In both objects, most variable is the central emission peak and the portion of the profile between about  $-100$  and  $-400 \text{ km s}^{-1}$ .

The same variations are seen in the P Cyg absorptions of the Na I D<sub>1,2</sub> lines, which correlate well with H $\alpha$ , although the Na I lines have a somewhat smaller range in wind velocity. The absorption at the infrared Ca II lines also vary together with H $\alpha$  and Na I but the velocity amplitude is much smaller. H $\alpha$  was chosen for analysis because it showed the largest range in wind velocity.

In FU Ori, the line profiles change considerably on a time scale of a day (as was noted most recently by D'Angelo et al. 2002a, who give earlier references). The following variability patterns are seen in the H $\alpha$  profile on SOFIN spectra: (1) There is no correlation between the changes of the absorption and emission components (we return to this matter in the following section). (2) Three sections of the absorption component vary independently of one another: (a) a “slow wind” at  $RV = -50$  to  $-110 \text{ km s}^{-1}$ , (b) a “fast wind” at  $-110$  to  $-270 \text{ km s}^{-1}$ , (c) an even faster wind at  $-270$  to  $-400 \text{ km s}^{-1}$ . (3) The fast wind portion shows quasi-periodic variations in EW, but (4) no periodicity is found in the emission component of H $\alpha$ .

The dense time coverage of the SOFIN spectroscopy makes feasible a search for periodicity, so the EW of the P Cyg absorption between  $-110$  and  $-270 \text{ km s}^{-1}$  was used as a parameter of the fast wind of FU Ori. Those EWs are listed in Table 8. The phase dispersion minimization method (Stellingwerf 1978) was used to search for periodicity in these data. When the velocities of only three seasons, 1997 to 1999, are examined (20 nights), the periodogram (Fig. 26, upper panel) shows a group of significant peaks at 13–18 days, with the most probable value being 14.847 days. Fisher's method of randomization (Nemec & Nemec 1985) gives a false alarm probability (FAP) of  $<0.01$  for that period. There are no other significant periods between 2 and 100 days. The phase diagram (Fig. 26, lower panel) shows that that period is defined largely by the 1997 and 1998 data. The data of 1999 also fit, but span a shorter phase interval. The periodicity is not present in the data of 2000 (7 nights) although the fast wind EW varied over almost the same range.

Errico, Vittone, & Lamzin (2003) have recently published H $\alpha$  profiles of FU Ori obtained over 5 consecutive nights in January 1999. The variations in the P Cyg absorption (measured by them as velocity width at an intermediate depth) indicated that if periodicity was present, the period could be about 6–8 days, shorter by a factor 2 than found from our more extended set of EW measurements. Considering that our observations in 2000 show no periodicity, it may be that the 14.8 day cycle had already become undetectable in 1999. Our own data of October 1999 (4 nights)

are too limited to pronounce upon the presence of a 6–8 day cycle in that year. We conclude that the variations of the wind absorption in FU Ori are quasi-periodic: in 1997–98 the period was 14.8 days but that periodicity had disappeared by 2000.

Errico et al. suggested that these cyclic variations in the wind of FU Ori are caused by the interaction of the stellar magnetic field with the disk outflow, assuming that the magnetic axis of the star is inclined to the disk rotational axis. However, in that model of an inclined magnetic rotator one would expect rather stable periodicity on a very long time scale. Instead, the *quasi-periodic* character of the variations is more like that observed in TTS, where surface inhomogeneities (spots) may appear and disappear due to changes in the star's magnetic field structure.

We suggest that the longer period of 14.8 days suggested by the H $\alpha$  variations (because that line showed the largest velocity amplitude) is the rotational period of FU Ori. In case the wind is governed by the star's magnetic field (as is believed to be the case in TTS), a relatively stable axial asymmetry of the field structure might cause the observed rotational modulation over at least two years (1997–98), or 50 rotational cycles. The observed  $v_{\text{eq}} \sin i = 70 \text{ km s}^{-1}$  then leads to a value of  $R \sin i = 20.4 \text{ R}_{\odot}$ .

In the accretion disk model for FU Ori (Kenyon et al. (1988)) a period of 14.8 days corresponds to a Keplerian orbit of radius  $20 \text{ R}_{\odot}$ , where the K-type spectrum is supposed to be formed, but it is not clear why a global disk wind should be modulated with any single period.

If the intrinsic optical colors of FU Ori are those of a normal G0 Ib, then the observed values for the 2000 season ( $V = 9.58$ ,  $V - R_J = +1.185$ ) correspond to  $E(V - R)_J = 0.575$ , so if the reddening is normal, the average  $A_V$  is 1.38 mag., leading to  $M_V = -0.1$  for the assumed distance of 450 pc. The visual flux in solar units is

$$\frac{F_V}{F_V(\odot)} = 2.512^{-M_V + M_V(\odot)} \quad (1)$$

If only a fraction  $x$  of the surface is occupied by regions having the G0 Ib brightness, then the radius of such a spherical star is

$$\frac{R}{R_\odot} = \left( \frac{F_V/F_V(\odot)}{xb} \right)^{1/2} \quad (2)$$

where  $b$  ( $= 0.7$ ) is the ratio of surface brightnesses at V calculated by the procedure of Barnes et al. (1976). If  $x = 1$ , the result is that  $R = 11.3 R_\odot$ .

Consider whether this last result can be reconciled with  $R \sin i = 20.4 R_\odot$ . If the star's surface brightness is not uniform, then any value of the coverage factor  $x \leq 0.32$  could bring the two into agreement, the inclination then following from  $\sin i = (20.4/11.3)x^{1/2}$ .

Another possibility: if the  $A_V$  inferred from the color excess of FU Ori were ignored and instead taken to be 2.66 mag., regarded as the sum of conventional interstellar reddening in the foreground and a circumstellar component of unspecified reddening properties, then  $M_V$  would become -1.3 and  $R = 20.4 R_\odot$ , in agreement with the axial rotation result for  $\sin i = 1$ . If the entire  $A_V$  was circumstellar, then  $A_V/E(B-V) = 5.4$ , compared to the normal interstellar value of 3.1. A/E ratios greater than about 4.0 are not unprecedented, having been found in dusty H II regions and in dense molecular clouds (Cardelli et al. 1989; Chini & Wargau 1998), there usually being ascribed to the presence of larger particles. That may not be inconceivable in the case of FU Ori because the local reddening of such a dusty object need not obey the normal interstellar extinction law. But there must surely be a normal interstellar contribution to  $A_V$ , in which case the A/E ratio of the circumstellar component would become even larger, as it also would if  $\sin i < 1.0$  for FU Ori.

So either hypothesis could reconcile the two results. We see no strong observational reason to favor one hypothesis over the other at this time, except that the dust explanation does require circumstellar extinction of unusual properties. The periodic variation in wind strength observed in FU Ori, with its implication of unevenly distributed active areas, favors the blotchy surface hypothesis. If precise photometry showed that FU Ori varies cyclically with that same period, it would strengthen that proposition. Dust formation low in the atmosphere, leading to a larger  $A_V$  and an abnormal A/E and subsequent ejection, might explain dust structure very near the star. But at this time the question remains open.

#### 4.4.2. Photospheric Profiles

As remarked earlier, the double-peaked profiles of (some) photospheric lines have been used as one of the arguments in support of the accretion-disk model of FUors (HK). So far, no spectral time series have been available to determine how stable is this peculiar line structure, which we attribute (§ 2.4) to the presence of emission cores in the low-excitation lines. In our spectral series of V1057 Cyg and FU Ori (SOFIN data of 1995–2001) this line structure is found to be variable on a time scale of several days. In the following we use the cross-correlation method to give information about line profiles averaged over a certain spectral region, usually one spectral order. The spectrum of  $\beta$  Aqr (G0 Ib) is used as a template.

As an example, Figures 27 and 28 show night-to-night variability of the cross-correlation functions (CCF's) during one set of observations of V1057 Cyg and FU Ori. The CCF profile varies synchronously in different spectral regions: the line width at half-depth remains about the same, while the central part varies with either shortward or longward peak being stronger, sometimes becoming single and quite symmetric. Of course the CCF profile depends on the particular mix of low- and high-excitation lines in the sample, and this may be why different spectral orders show somewhat different CCF shapes, but the variations are similar in different orders. The spectral intervals selected for cross-correlation were chosen to avoid lines with shell components.

As a descriptor of line position we use the “center of gravity” of the CCF, namely its weighted mean radial velocity. This is the velocity of the star as if it had been measured from the “center of gravity” of a photospheric line profile, although variations of this quantity do not necessarily mean that the whole star moves around in radial velocity.

In the case of V1057 Cyg two spectral orders (6320–6440 and 6575–6640 Å) were combined; the resulting precision of RV is about  $\pm 3$  km s<sup>-1</sup>. The spectra of FU Ori are of better quality, so 6 spectral orders (from 5560 to 7520 Å) were used, the resulting precision being  $\pm 1$  km s<sup>-1</sup>. Table 9 contains the measured RV's for both stars.

Since the individual CCFs are quite noisy, especially for V1057 Cyg, three groups of CCFs show-

ing similar RVs were selected: shortward-shifted, centered, and longward-shifted. The three CCFs shown in Figure 29 are averages for these three groups, overplotted to illustrate typical variations of the CCF profile. For V1057 Cyg each CCF is an average of 8 spectra, for FU Ori each is an average of four. Obviously, the main source of the variability is the deformation of the central part of the line profile: the ratio of shortward-to-longward peak intensity is variable, while the width of the line remains about the same. This latter fact excludes the possibility of a double-line binary, where the line width must be narrower when the two components have the same radial velocity.

For FU Ori, the periodogram shown in the upper panel of Figure 30 was calculated using the data of the 1997, 1998 and 1999 seasons (20 nights). The most probable period is 3.542 days, with  $\text{FAP} < 0.01$ . When phased with this period, the lower panel of Figure 30 shows the cyclic variation of RV in these three years. The semi-amplitude of the sinusoidal variations of RV is  $1.8 \text{ km s}^{-1}$ . The scatter of points around the sinusoidal curve is less than  $\pm 1 \text{ km s}^{-1}$ , which must be entirely due to the errors in RV. When all the data of 1995–2000 are used (29 nights), the period is still present but the data of 2000 are not well fit to the sinusoidal curve. It is concluded that the period of 3.542 days in the photospheric lines of FU Ori was stable during at least three years.

For V1057 Cyg, using all the data of 1995–2001 (42 nights), the periodogram reveals a group of peaks around 4.4–4.5 days, with the most probable period being 4.43 days. However, the semi-amplitude of the RV variations ( $3 \text{ km s}^{-1}$ ) is comparable to the errors in RV ( $3 \text{ km s}^{-1}$ ), which makes it unlikely that the periodicity is real, so we draw no conclusions from this result.

The nature of such variations in the photospheric line structure is not clear. In the case of a single star, variations like those shown in Figure 29 can be caused by an asymmetric polar starspot. However, a dark spot must also modulate the apparent stellar brightness. No such variation has been reported for FU Ori. Since the photospheric line doubling is due to the presence of emission cores, variations in the doubling may be caused by movement of those cores. It is also possible that the line emission originates from a volume of gas distributed non-axisymmetrically around the star.

Such “emission spots” could also produce a rotational modulation of the photospheric line profile. On the other hand, if the wind cycle of 14.8 days is the rotational period, it is hard to explain why the period of the photospheric variations is 4 times shorter.

In case of the accretion disk model (Kenyon et al. 1988), a period of 3.542 days corresponds to Keplerian rotation at a distance of  $7.7 R_\odot$  (if the mass of the central star is  $0.5 M_\odot$ ). This is the innermost part of the disk, where the F-type spectrum is supposed to be formed. If variability of the photospheric lines is caused by some kind of brightness asymmetry in the disk, the stability of such an asymmetry over three years (300 orbital periods) would be difficult to understand in a differentially rotating disk.

Apart from the deformation of the line profiles, small shifts of the CCF can be noticed in V1057 Cyg (Fig. 29): the change in the shortward-to-longward peak intensity is accompanied by shifts of the entire CCF profile by a few  $\text{km s}^{-1}$ . If these shifts are real, and not an artifact of cross-correlating noisy spectra, it could indicate the presence of a low mass secondary near the star. Series of better quality spectra are needed to check whether this effect is really present.

Unruh, Collier Cameron, & Guenther (1998) have inferred the presence of hotspots on the rotating TTS DF Tau by an analysis of such cyclic deformations of absorption line profiles. Those hotspots, which they suggest are accretion shocks at mass-infall points, are clearly hotter than any of those on the classical FUors, where there is no sign of the He I lines at 5875 or 7065 Å in emission.

#### 4.5. Infall

Our new spectroscopic material refutes a concern that we raised in 1992, namely that there was then no direct spectroscopic evidence of infall in FUors, such as “reversed P Cyg” structure. Disk theory yields an accretion rate onto the FUor central star of about  $10^{-4} M/M_\odot \text{ yr}^{-1}$  (Hartmann & Kenyon 1996), as compared to  $\approx 10^{-7} M/M_\odot \text{ yr}^{-1}$  for classical T Tauri stars (CTTS). One would think that the movement of such massive amounts of material on to the star would surely be detectable.

The disk hypothesis has been extensively elabo-

rated since HK and a number of possible explanations have been offered for the lack of evidence for infall: (a) much of the accreted material may be ejected from the disk surface as wind, and so never reaches the star; or (b) the accreting mass may accumulate in the disk; or (c) the central source may be so faint that absorption lines would not be detectable against its continuum; or (d) the disk may be so thick at its inner edge that any activity nearer the star is concealed (in fact Kley & Lin [1996] predict that at an accretion rate of  $10^{-4} M/M_\odot \text{ yr}^{-1}$  "the entire stellar surface is engulfed by opaque disk gas"); or (e) an optically thin infall region may be hidden not because of disk thickness but because these FUors are observed at unfavorable aspect angles.

However, as a result of the detailed time coverage at SOFIN, evidence of what appears to be sporadic infall onto the continuum source can now be seen in the  $H\alpha$  profiles of both FU Ori and V1057 Cyg. On two (of 29) SOFIN spectra a weak absorption component appeared at about  $RV = +90 \text{ km s}^{-1}$  in the longward wing of  $H\alpha$ . Figure 31 shows three of these spectra, demonstrating that the feature was present on JD 2450796.68, but not at comparable strength on the day before or two days later. The pattern was the same at  $H\beta$ , and the absorption was marginally detectable at the  $\text{Na I } D_{12}$  lines, but not at the  $\text{O I } \lambda 7773$  blend which in CTTS is sensitive to accretion. A similar absorption had appeared at  $H\alpha$  at about the same velocity on JD 2450807.69, but had been absent on the day before. Clearly, these infall features in FU Ori vary rapidly in strength, on a time scale of one day or less. The longward wing of the absorption in  $H\alpha$  extends to about  $+150 \text{ km s}^{-1}$ , which is near the free fall velocity at the surface of a star of 1 solar mass and a radius of  $20 R_\odot$ . A similar event has been seen in a HIRES observation of FU Ori in early 2003.

It is uncertain if the complete suppression of the longward component of  $H\alpha$  as seen in the right-hand panel of Figure 25 can be ascribed to very heavy accretion of this kind.

Thus infalling material does appear sporadically in the line of sight to both FU Ori and V1057 Cyg, as is observed in many CTTS (Edwards, Hartigan, Ghandour, & Andrulis 1994). It is there thought to be due to magnetically-channeled, free-falling disk material. A signature of such magneto-

spheric accretion is the presence of emission lines of He I and He II that are believed to originate in the hot spots where infalling material impacts the star (Beristain, Edwards, & Kwan 2001). As already noted, no such emission lines appear in any of our spectra of the classical FUors.

It has been suggested that in CTTS a consequence of such infall may be the ejection of Herbig-Haro-like jets, and it is interesting that the spacing of structure in some H-H outflows does correspond to estimates of the time spacing of repetitive FUor events in TTS. A signature of such shocked gas is the presence of lines of [O I], [S II] and sometimes [N II] (Cabrit et al. 1990). All that we have found in the integrated spectra of the FUors that we have observed are the very weak, broad [O I] and [Fe II] emissions in V1057 Cyg (§ 2.4). They have large negative velocities and so must be formed in the outflowing wind. The [S II] or [N II] lines are not detected, although they would be expected to be much weaker. However, no H-H-like jets are seen in the direct images of the FUors we have observed, although a search at higher angular resolution with the proper filters would be worthwhile.

#### 4.6. The Ca II H and K lines in FUors

An unusual feature of the pre-outburst spectrum of V1057 Cyg was that although the K line ( $\lambda 3933$ ) of Ca II was strong in emission, the H line ( $\lambda 3968$ ) was absent. The obvious explanation of this oddity, as was realized long ago, is that  $\lambda 3968$  is quenched by the P Cyg absorption component of  $\text{He } \lambda 3970$ . The important conclusions are (a) that 12 years *before* the 1970 flare-up, V1057 Cyg was subject to a strong mass outflow: i.e. the high-velocity wind did not turn on at the time of the outburst; and (b) that wind was seen against the spectrum of the pre-outburst star.

The same anomaly was also present 28 years *after* the flare-up: a HIRES spectrogram obtained 1998 October 30, when the star was about 1 mag. (in B) above minimum brightness, is shown in Fig. 32. It demonstrates not only that the  $\text{He}$  wind is indeed responsible for the K:H anomaly, but implies that such a wind may be a quasi-permanent characteristic of the object.

This same wind suppression of Ca II  $\lambda 3968$  has been observed in FU Ori since the time of the first adequate spectroscopy (1948). It is seen not only

in the other classical FUor that we have observed (V1515 Cyg) but also in Z CMa which has been called a FUor, as well as in V1331 Cyg to which attention was called long ago by Welin (1971) for that very reason. Only BBW76 (Reipurth 1990, 1997, 2002) does not conform: narrow emission is present in both Ca II lines. Figure 32 shows HIRES spectra of the 3900–3980 Å region for all 6 stars. The presence of strong Ca II emission in all the FUors, both near or below maximum light, shows that a permanent chromosphere is characteristic of the group.

This K:H anomaly is not a common feature of TTS spectra. Most TTS outflows occur at modest negative velocities such that the absorption component at H $\alpha$  falls within the broad underlying emission line: see the atlases of H $\alpha$  profiles by Fernández et al. (1995) and by Reipurth, Pedrosa, & Lago (1996). FUor outflows are dramatically different, in that the mass involved is much larger and extends to much greater negative velocities, hence the characteristic P Cyg profile and the suppression of H $\epsilon$ . If this K:H anomaly is indeed a FUor signature, can it be that there are unrecognized FUors among the host of ordinary TTS? There are 65 stars with Ca II emission in the atlas of TTS spectra by Valenti, Basri, & Johns (1993) and of these only 3 (AS 353A, LkH $\alpha$  321, V1331 Cyg) have the Ca II  $\lambda$ 3968 line suppressed. The spectra of 3 additional stars apparently showing the same effect have been published by Pereira et al. (2001). Detection of such stars by slitless spectroscopy would be an efficient means of searching for new FUor candidates.

#### 4.7. Does the FUor Phenomenon Occur in Every T Tauri Star?

Before the 1970 outburst, V1057 Cyg was only one of some fifty faint H $\alpha$ -emission stars scattered over the NGC 7000-IC 5070 region. Since it seemed to be just another TTS—on the slender evidence of that single pre-outburst low-resolution slit spectrogram—it was suggested in Herbig (1977) and then again in Herbig (1989) that such outbursts might be a characteristic of TTS in general. If so, from the number of such outbursts that had been detected (3 at that time) and a guess as to how many TTS exist within an observable distance around the Sun, it was estimated that “the mean time between suc-

sive FU Ori-like outbursts in an individual T Tau star” is about  $10^4$  years. That estimate has since been refined by others but the basic concept has survived.

As appealing as that idea is, and the way it can be worked into a larger picture of pre-main sequence evolution (Hartmann & Kenyon 1996), it was a pure conjecture. Consider these points:

First, if every TTS is a potential and presumably recurrent FUor, then FUors would be expected to appear in clusters or associations rich in TTS. None of the classical FUors occur in the Orion Nebula, around  $\rho$  Oph, or in other regions containing large numbers of TTS. V1057 Cyg lies in an isolated dark cloud containing only one other very faint H $\alpha$  emitter,<sup>8</sup> no other TTS have been found in the elongated streamer northwest of IC 5146 where V1735 Cyg is located, while V1515 Cyg is one of several H $\alpha$  emitters scattered over an extended obscured region. BBW76 is alone in a small dark cloud, with no known TTS in the vicinity. There are exceptions, however: there are a number of TTS near the small dark cloud B35 in which FU Ori lies, and the heavily obscured L1551 IRS 5 is located in a loose grouping of TTS at the southern edge of the Taurus clouds. Another possible exception may be the candidate FUor CB34V which, according to Alves & Yun (1995), appears to lie on the near side of a heavily obscured aggregate of young stars.

Second, it was pointed out above (§ 4.6) that at minimum light, some 12 years before the outburst, V1057 Cyg exhibited the same strong outflowing wind that it has shown ever since the flare-up. The same P Cyg structure at H $\alpha$  is found in other FUors observed near maximum light. Such vigorous mass ejection is not a property of ordinary TTS, which is the reason it has become to be regarded as an indicator of FUor group membership.

Third, others have noted that FUors tend to have large values of  $v_{\text{eq}} \sin i$ . Even higher than the  $v_{\text{eq}} \sin i$ ’s found here for V1057 Cyg (55 km s $^{-1}$ ) and FU Ori (70 km s $^{-1}$ ) is the  $145 \pm 20$  km s $^{-1}$  reported by Alves et al. (1997) for the candidate FUor CB34V. FUors clearly have significantly higher rotational velocities than most TTS,

<sup>8</sup>It is the star arrowed in Figure 1a of Duncan, Harlan, & Herbig (1981).

although a minority of TTS are also rapid rotators: four of some 60 TTS listed by Hartmann & Stauffer (1989) and by Bouvier et al. (1986) have  $v_{\text{eq}} \sin i > 50 \text{ km s}^{-1}$ . We are encouraged to believe that rapid rotation is an essential characteristic of the FUor phenomenon.

There is another property that, at first, would seem to distinguish FUors from most conventional TTS. Goodrich (1987) noted that all the FUors recognized at that time were located at the edge of either a complete loop or ring of reflection nebulosity; in some cases only a section of the loop is seen as a curved arc terminating at the star. In addition to the well-known outer arcs at V1057 Cyg, the HST images in Figure 15 show two curved filaments (A and B) that could be part of such a recently ejected loop. Interestingly, V1331 Cyg and Z CMa (both of which show the K:H anomaly), as well as BBW76 are also attached to such nebulae. But so are seemingly unrelated stars like SU Aur and AB Aur ( $v_{\text{eq}} \sin i$  about  $65 \text{ km s}^{-1}$  and  $80 \text{ km s}^{-1}$ , respectively), showing that the presence of such a nebula is not exclusively a FUor signature, but may rather be the consequence of a very large  $v_{\text{eq}}$ .

These reasons encourage the speculation that FUor events may not be a property of ordinary TTS, but may be confined to a special rapidly rotating sub-species among them. But if the FUor phenomenon is in fact favored in a certain kind of pre-main sequence object, it raises the question: what could be special about stars that so often occur in isolation, in contrast to those formed in groups or clusters?

## 5. Summary and Conclusions

In Petrov & Herbig (1992), following a study of a high-resolution spectrogram of FU Ori obtained in 1987, we asserted that that spectrum could be reproduced by an emission-line shell (which in the present paper we call a ‘chromosphere’) overlain by a rising, cooler absorbing layer (now the ‘shell’) atop a G-type supergiant absorption spectrum whose lines were broadened by macroturbulence + rotation. It was also pointed out that some of the spectroscopic properties of FUors that have been argued as proof of the accretion disk picture (line doubling, the presence of CO bands in the near infrared, the possession of an IR excess) are

found in a number of much older high-luminosity stars where there is no reason whatsoever to think that an accretion disk is present.

The new SOFIN and HIRES spectroscopy was intended to reexamine those assertions. With respect to the three issues critical to the accretion disk hypothesis that were raised in § 1, our conclusions are:

(a) The emission cores responsible for the ‘doubling’ of low-excitation absorption lines that have become more apparent as V1057 Cyg has faded clearly are produced in a low-temperature chromosphere. We believe that it is they that caused those absorption lines to appear double when the star was brighter. Presumably such chromospheres are present in the other classical FUors as well, judging from the ubiquity of Ca II  $\lambda 3933$  emission.

(b) We have been unable to confirm, with superior spectroscopic material, the dependence of  $v_{\text{eq}} \sin i$  upon either wavelength or lower EP that has been urged as evidence for the accretion disk model. However we do agree that the CO lines in the  $2 \mu\text{m}$  region of FU Ori are narrower than are optical lines shortward of  $0.9 \mu\text{m}$ ; the situation for V1057 Cyg is uncertain. Whether this is unarguable support for the disk hypothesis is not clear: it would be interesting to determine if the same effect appears in the CO lines of normal G supergiants.

(c) Synthetic disk spectra that resemble FUors at optical wavelengths fail to match certain critical lines in the near infrared, indicating that syntheses such as those described in § 4.1 can no longer be regarded as firm support for the disk hypothesis, although some elaboration of that hypothesis might reduce the discrepancies.

The point is that we find that some of the *observational* evidence that has been offered in support of the disk hypothesis can either be explained in another way or cannot be confirmed. Although details are somewhat different, the proposal of Petrov & Herbig (1992) and of Herbig (1989) is strengthened: namely, that the observable properties of the classic FUors are better explained by a single star rotating near the limit of stability and losing mass via a powerful wind, as was originally proposed by Larson (1980).

On slender evidence, V1057 Cyg is assumed to

have been a classical TTS before the 1970 outburst. Although by 1999 it had declined to about 1.5 mag. (in B) above minimum, the spectrum still (by 2002) has not begun to resemble that of a conventional CTTS. In time it may do so, and some of the issues raised here may be resolved. Meanwhile, it is important that the star be monitored spectroscopically on a regular basis.

We are much indebted to the late V. Shevchenko and to M. Ibrahimov for providing us with their FUor photometry, to Keith Budge, Lee Hartmann, Ken Hinkle and Karl Stapelfeldt for material which we have found very useful in the course of this investigation, to Ted Simon for assistance with the CO data, to Ilya Ilyin for assistance with the SOFIN observations, and to Bo Reipurth for helpful comments. The work of G.H. on FUors has been partially supported by the U.S. National Science Foundation under Grants AST 97-30934 and 02-04021. The work of P.P. and R.D. was supported by the EC Human Capital and Mobility Network project “Late-type Stars: activity, magnetism, turbulence,” and of P.P. by the CAUP grant “Financiamiento Plurianual.”

## REFERENCES

Alves, J. F., & Yun, J. L. 1995, *ApJ*, 438, 107

Alves J., Hartmann, L., Briceño, C., & Lada, C. J. 1997, *AJ*, 113, 1395

Barnes, T. G., Evans, D. S., & Parsons, S. B. 1976, *MNRAS*, 174, 503

Bastien, U., & Mundt, R. 1985, *A&A*, 144, 57

Bell, K. R. 1999, *ApJ*, 526, 411

Bell, K. R., Lin, D. N. C., Hartmann, L. W., & Kenyon, S. J. 1995, *ApJ*, 444, 376

Beristain, G., Edwards, S., & Kwan, J. 2001, *ApJ*, 551, 1037

Bouvier, J., Bertout, C., Benz, W., & Mayor, M. 1986, *A&A*, 165, 110

Cabrit, S., Edwards, S., Strom, S. E., & Strom, K.M. 1990, *ApJ*, 354, 687

Cardelli, J. A., Clayton, G. C., & Mathis, J. S. 1989, *ApJ*, 345, 245

Chini, R., & Wargau, W. F. 1998, *A&A*, 329, 161

Clarke, C. J., Lin, D. N. C., & Pringle, J. E. 1990, *MNRAS*, 242, 439

Croswell, K., Hartmann, L., & Avrett, E. H. 1987, *ApJ*, 312, 227

D’Angelo, G., Errico, L., Gomez, M. T., Smaldone, L. A., Teodorani, M. & Vittone, A. A. 2000b, *A&A*, 356, 888

D’Angelo, G., Gomez, M. T., Errico, L., Smaldone, L. A., & Vittone, A. A. 2000a, *Mem. Soc. Astr. Ital.*, 71, 1037

Draine, B. T. 1985, *ApJS*, 57, 587

Duncan, D. K., Harlan, E. A. & Herbig, G. H. 1981, *AJ*, 86, 1520

Edwards, S., Hartigan, P., Ghandour, L., & Andrusilis, C. 1994, *AJ*, 108, 1056

Elias, J. H. 1978, *ApJ*, 223, 859

Errico, L., Vittone, A. A. & Lamzin, S. A. 2003, in press

Fernández, M., Ortiz, E., Eiroa, C., & Miranda, L. F. 1995, *A&AS*, 114, 439

Goodrich, R. W. 1987, *PASP*, 99, 116

Haro, G. 1971, *Inf. Bull. Var. Stars* 565

Hartmann, L., & Calvet, N. 1995, *AJ*, 109, 1846

Hartmann, L., & Kenyon, S. J. 1985, *ApJ*, 299, 462 (HK)

Hartmann, L., & Kenyon, S. J. 1987a, *ApJ*, 312, 243

Hartmann, L., & Kenyon, S. J. 1987b, *ApJ*, 322, 393

Hartmann, L., & Kenyon, S. J. 1996, *ARA&A*, 34, 207

Hartmann, L., & Stauffer, J. R. 1989, *AJ*, 97, 873

Herbig, G. H. 1958, *ApJ*, 128, 259

Herbig, G. H. 1977, *ApJ*, 217, 693

Herbig, G. H. 1989, in ESO Workshop on Low-Mass Star Formation and Pre-Main Sequence Objects, ed. B. Reipurth (Garching: ESO), 233

Herbig, G. H. 1990, *ApJ*, 360, 639

Hinkle, K. H., Cuberly, R., Gaughan, N., Heynssens, J., Joyce, R., Ridgway, S., Schmitt, P., & Simmons, J. E. 1998, *Proc. SPIE*, 3354, 810

Ibrahimov, M. 1996, *IBVS* No. 4285

Ibrahimov, M. 1999, *IBVS* No. 4691

Kenyon, S. J., Hartmann, L., & Hewett, R. 1988, *ApJ*, 325, 231

Kenyon, S. J., Hartmann, L. W., & Kolotilov, E. A. 1991, *PASP*, 103, 1069

Kenyon, S. J., Kolotilov, E. A., Ibragimov, M. A., & Mattei, J. A. 2000, *ApJ*, 531, 1028

Kley, W., & Lin, D. N. C. 1996, *ApJ*, 461, 933

Kley, W., & Lin, D. N. C. 1999, *ApJ*, 518, 833

Kolotilov, E. A., & Kenyon, S. J. 1997, *IBVS* No. 4494

Kopatskaya, E. N. 1984, *Astrofiz.*, 20, 263

Kopatskaya, E. N., Grinin, V. P., Shakhovskoy, D. N., & Shulov, O. S. 2002, *Astrofiz.*, 45, 175

Laakkonen, T. 2000, in *Proc. 33rd ESLAB Symp.*, ed. F. Favata, A. A. Kaas, & A. Wilson, *ESA SP-445* (Noordwijk, The Netherlands: ESA), 445

Larson, R. B. 1980, *MNRAS* 190, 321

Laugalys, V., & Straižys, V. 2002, *Baltic Astr.*, 11, 205

Lobel, A., Israeliyan, G., de Jager, C., Musaev, F., Parker, J. W., & Mavrogiorgou, A. 1998, *A&A*, 330, 659

Malbet, F., et al. 1998, *ApJ*, 507, 149

McMuldroch, S. 1995, PhD thesis, California Institute of Technology, p. 72

Mendoza, E. E. 1972, *ApJ*, 169, L117

Mould, J. R., Hall, D. N. B., Ridgway, S. T., Hintzen, P., & Aaronson, M. 1978, *ApJ*, 222, L123

Nakajima, T., & Golimowski, D. A. 1995, *AJ*, 109, 1181

Nemec, A. F. L., & Nemec, J. M. 1985, *AJ*, 90, 2317

Pereira, C. B., Schiavon, R. P., de Araújo, F. X., & Laudaberry, S. J. C. 2001, *AJ*, 121, 1071

Petrov, P. P., & Herbig, G. H. 1992, *ApJ*, 392, 209

Petrov, P., Duemmler, R., Ilyin, I., & Tuominen, I. 1998, *A&A*, 331, L53

Petrov, P. P., et al. 2001, *A&A*, 369, 993

Porter, J. M. 1996, *MNRAS*, 280, L31

Rao, N. K., et al. 1999, *MNRAS*, 310, 717

Reipurth, B. 1990, in *IAU Symp. 137, Flare Stars in Star Clusters, Associations and the Solar Vicinity*, ed. L. V. Mirzoyan, B. R. Petterson, & M. K. Tsvetkov (Dordrecht: Kluwer), 229

Reipurth, B., Pedrosa, A., & Lago, M. T. V. T. 1996, *A&AS*, 120, 229

Reipurth, B. 1997, in IAU Symp. 182 (poster proceedings), Low Mass Star Formation from Infall to Outflow, ed. F. Malbet & A. Castets (Grenoble: Laboratoire d'Astrophysique, Observatoire de Grenoble), 309

Reipurth, B., Hartmann, L., Kenyon, S. J., Smette, A., & Bouchet, P. 2002, AJ, 124, 2194

Rieke, G., Lee, T., & Coyne, G. 1972, PASP, 84, 37

Rustamov, B. N. 2001, Astrophys. Lett., 27, 34

Sargent, W. L. W. 1961, ApJ, 134, 142

Stellingwerf, R. F. 1978, ApJ, 224, 953

Tuominen, I., Ilyin, I., & Petrov, P. 1999, in Astrophysics with the NOT, Proceedings of the Conference held in Turku in August 12–15, 1998, ed. H. Karttunen, & V. (Piikkio, Finland: University of Turku, Tuorla Observatory), 47

Unruh, Y. C., Collier Cameron, A., & Guenther, E. 1998, MNRAS, 295, 781

Valenti, J. A., Basri, G., & Johns, C. M. 1993, AJ, 106, 2024

Wallace, L., & Hinkle, K. 1996, ApJS, 107, 312

Wallace, L., & Hinkle, K. 1997, ApJS, 111, 445

Welin, G. 1971, A&A, 12, 312

Welty, A. D., Strom, S. E., Strom, K. M., Hartmann, L. W., Kenyon, S. J., Grasdalen, G., & Stauffer, J. R. 1990, ApJ, 349, 328

Welty, A. D., Strom, S. E., Edwards, S., Kenyon, S. J., & Hartmann, L. W. 1992, ApJ, 397, 260

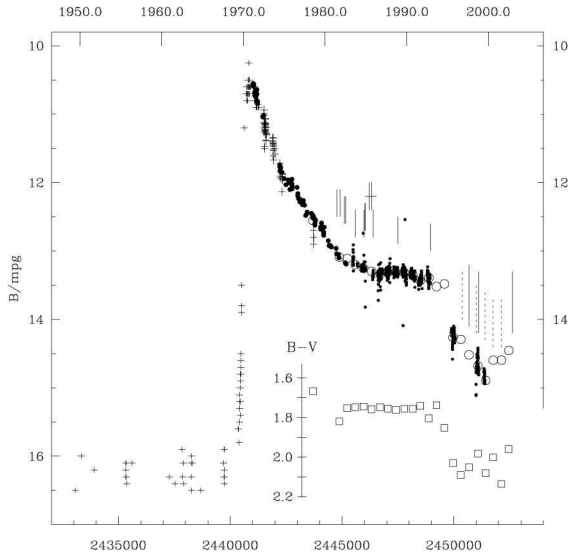


Fig. 1.— The B/pg light curve of V1057 Cyg. Crosses represent photographic observations, solid points are photoelectric or CCD magnitudes, open circles are seasonal averages (from Ibrahimov 1996, 1999, and private communication). The vertical lines mark the dates of high-resolution spectroscopic observations: short lines by the CfA group or others at KPNO, long dashed lines by Petrov with NOT/SOFIN, long solid lines by Herbig with HIRES. The two short lines with cross-bars represent the dates of the two Lick spectrograms of 1985. The lower section shows, as small squares, the seasonal average  $B - V$ 's, again from Ibrahimov. The increase in reddening in 1994-95 coincided with an abrupt drop in brightness.

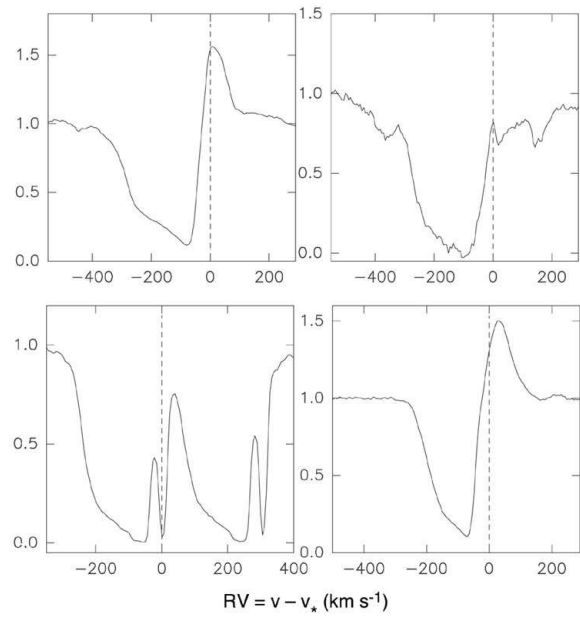


Fig. 2.— P Cyg structure of the H $\alpha$  (upper left), H $\beta$  (upper right), Na I D $_{1,2}$  (lower left) and Ca II  $\lambda 8542$  (lower right) lines in V1057 Cyg from the SOFIN spectra of 1997 August.

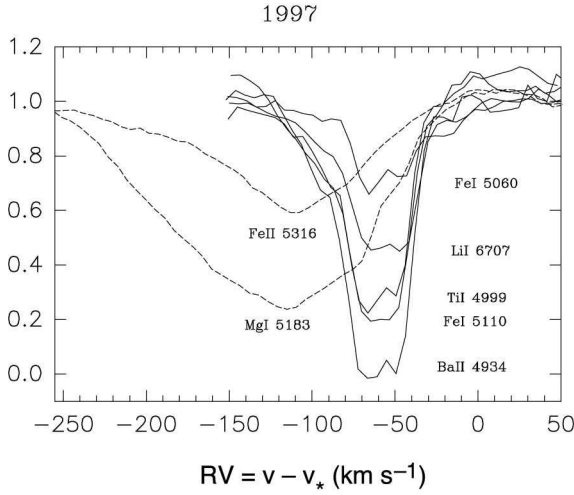


Fig. 3.— V1057 Cyg shell lines in 1997, from SOFIN spectra of 13 km s<sup>-1</sup> resolution. The spectrum of  $\beta$  Aqr, spun up to 55 km s<sup>-1</sup> and veiled by a factor 0.3, has been subtracted. The velocity scale is in the stellar rest frame. Low excitation lines (EP < 1 eV) are shown by solid lines, higher excitation lines (2-3 eV) are dashed. The strong lines of higher excitation potential, as Mg I  $\lambda$ 5183 and Fe II  $\lambda$ 5316, have as well shortward-shifted components at large velocities, about -120 km s<sup>-1</sup>.

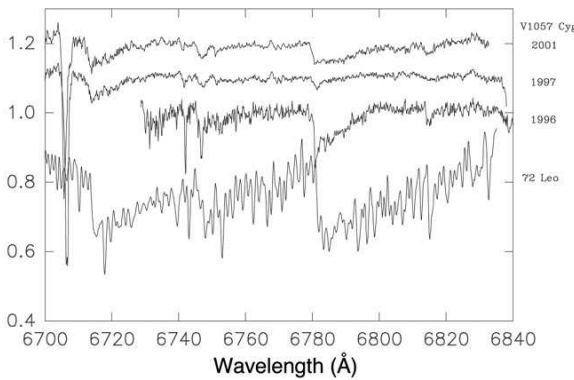


Fig. 4.— The shell TiO bands in the spectrum of V1057 Cyg in 1996, 1997, and 2001. The photospheric spectrum has been subtracted. The strong absorption near 6706 is the Li I shell component. The lowermost curve is the spectrum of 72 Leo (M3 IIb).

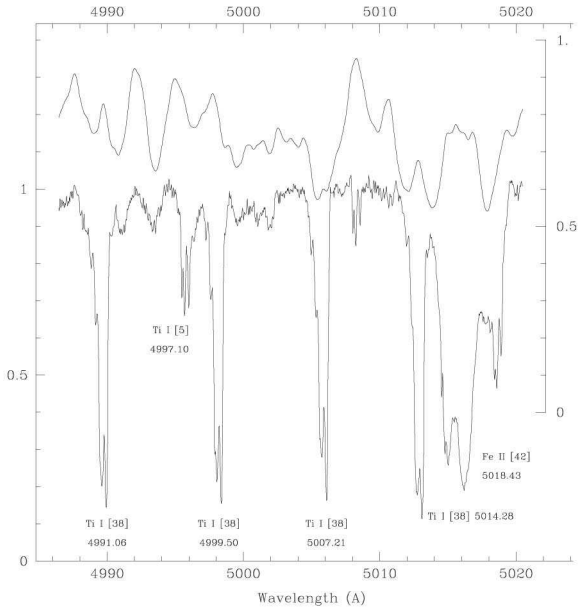


Fig. 5.— The 4990-5020 Å region in V1057 Cyg, from the HIRES spectrogram of 1997 August 12 (scale on the left), showing the strong shell lines of Ti I. Square brackets enclose their RMT multiplet numbers. The upper panel (scale on the right) is the same region in HD 190113 (type G5 Ib) broadened by  $v_{\text{eq}} \sin i = 55$  km s<sup>-1</sup>.

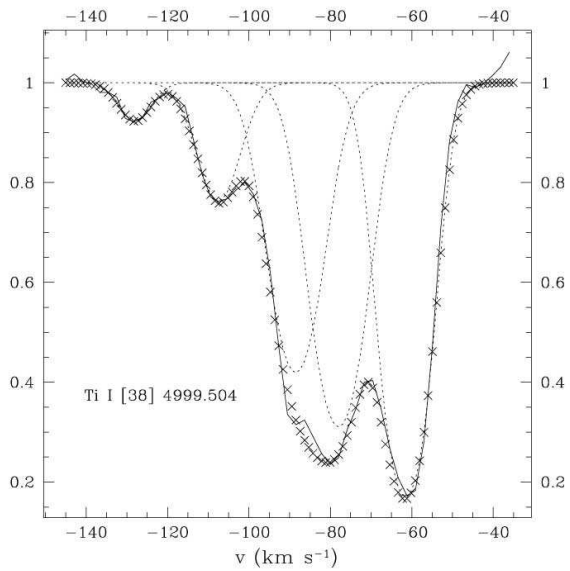


Fig. 6.— Example of the resolution of the shell components of Ti I  $\lambda$ 4999.504 by the procedure of § 2.3. The dotted lines outline the gaussians fitted to each of the 5 components, the crosses their sum, the solid line the observed profile.

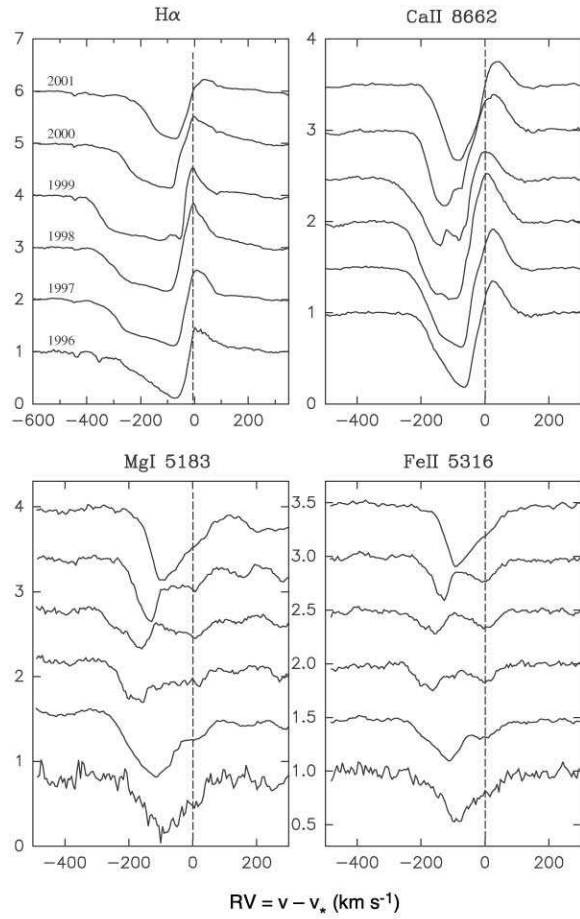


Fig. 7.— Star and shell line profiles during the 1996–2001 brightness minimum of V1057 Cyg.

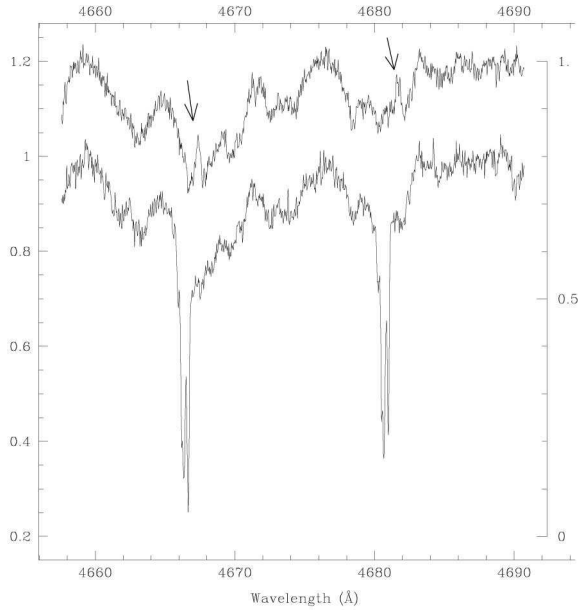


Fig. 8.— The 4660–4690 Å region in V1057 Cyg from HIRES spectrograms of 1997 August 12 (below, scale on the left) and 1998 October 30 (above, scale on the right). Between those dates the shell spectrum had essentially disappeared, illustrated here by the 4667 and 4681 Å shell lines of Ti I. In these and many others, narrow emission components (here arrowed) at approximately the stellar velocity became apparent when the complex shell absorption lines vanished.

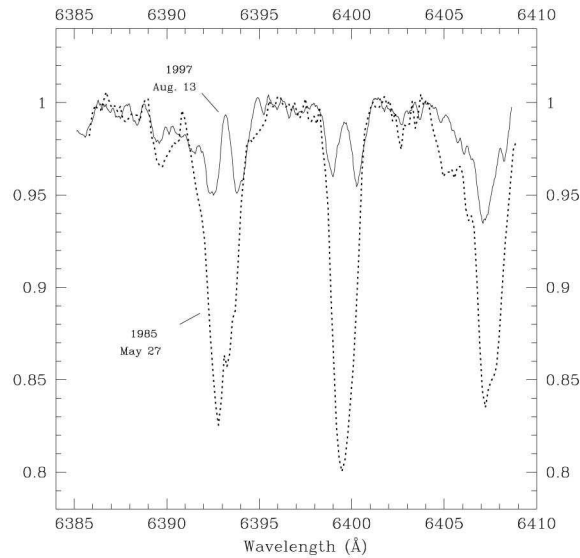


Fig. 10.— The 6385–6408 Å region in V1057 Cyg, from a Lick CCD spectrogram of 1985 May 27 (dotted) and from a HIRES spectrogram of 1997 August 13 (solid line); the latter has been smoothed by a 3-pixel box. In the intervening 12 years the centers of the 6393, 6400 Å Fe I absorptions have become emission lines, with peak intensities nearly at continuum level.

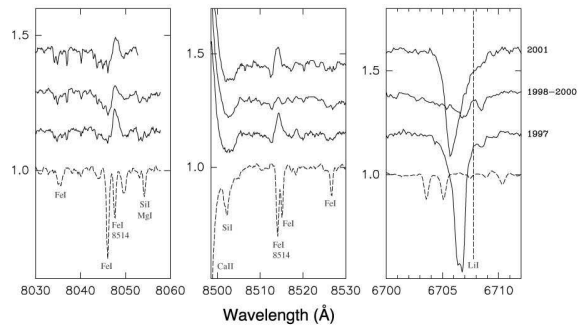


Fig. 9.— Emission lines of Fe I  $\lambda$ 8047 and Fe I  $\lambda$ 8514 in V1057 Cyg at three epochs (solid). The template spectrum of  $\beta$  Aqr is at the bottom (dotted). The vertical line marks the position of the Li I  $\lambda$  6707 line in the V1057 Cyg stellar rest frame.

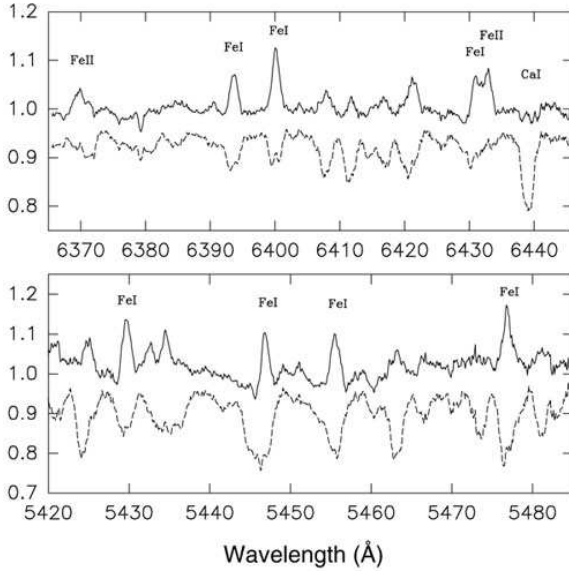


Fig. 11.— Two sections of the differential spectrum (solid line) obtained as a difference between that of V1057 Cyg (dashed line) and the template spectrum of  $\beta$  Aqr, spun up to  $55 \text{ km s}^{-1}$  and veiled by 0.3.

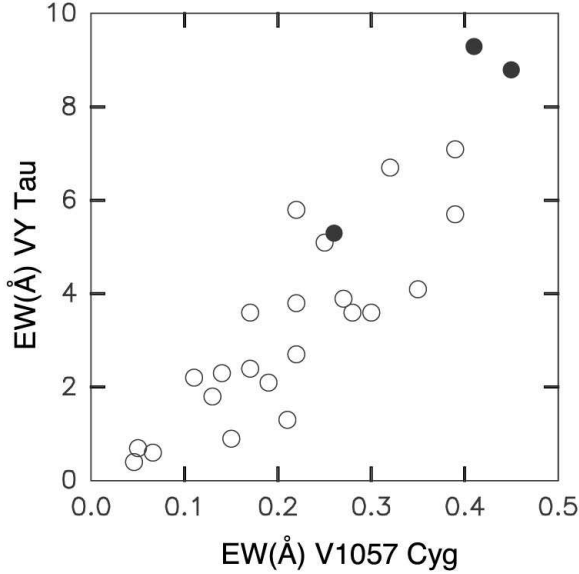


Fig. 12.— Correlation between equivalent widths of emission lines in V1057 Cyg and VY Tau. Filled circles: the “true” emission lines seen above the continuum level in V1057 Cyg. Open circles: the emission lines revealed in the differential spectrum of V1057 Cyg.

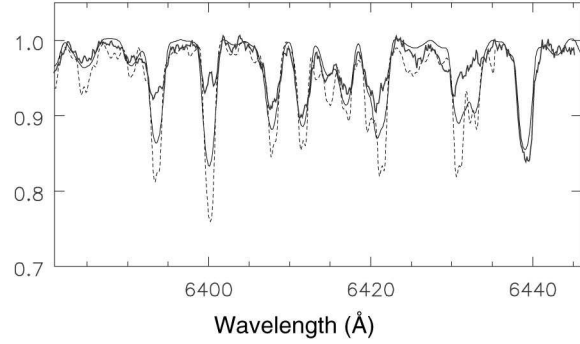


Fig. 13.— Photospheric lines in the average spectrum of V1057 Cyg in 1998–2000 (solid line). Shown for comparison are the spectrum of  $\beta$  Aqr, spun up to  $v_{\text{eq}} \sin i = 55 \text{ km s}^{-1}$  and veiled by 0.3 (thin line), and the synthetic spectrum of the accretion disk (dashed line), calculated according to Kenyon et al. (1988).

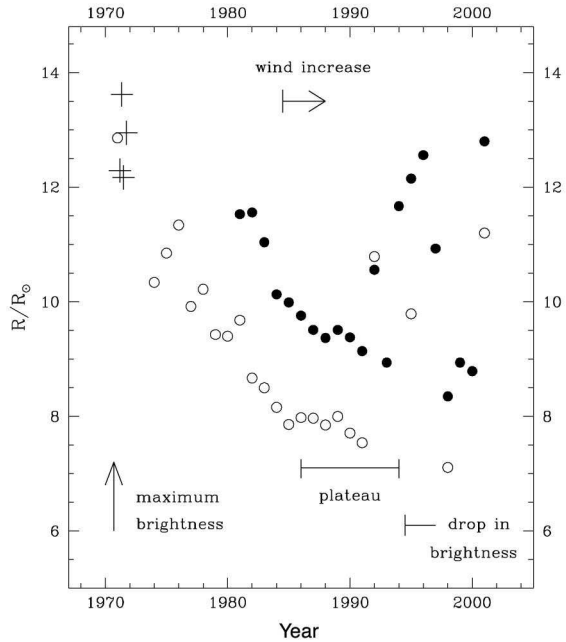


Fig. 14.— The variation of radius (in solar units) of V1057 Cyg from maximum light until 2001, calculated from  $V$ ,  $(V-R)_J$  observations of Kopatskaya et al. (2002): open circles; Ibrahimov (1996, 1999, priv. comm.); filled circles; and Mendoza (1972) and Rieke et al. (1972): crosses.

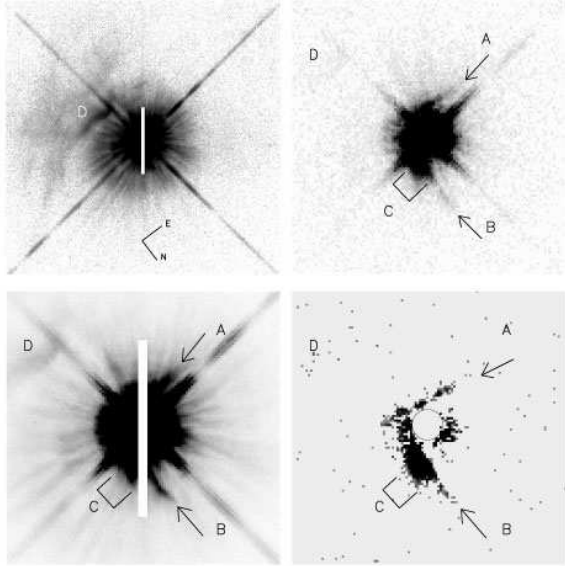


Fig. 15.— Hubble Space Telescope images of V1057 Cyg, obtained with WFPC2 on 1999 October 18 and filter F606W (central wavelength 5957 Å). Upper left: an average of two 180 s exposures on a logarithmic intensity scale. The white bar conceals the detector bleeding of the star image; it is 3''.5 long. The field size is 14''.6 square. Upper right: an area of 5''.5 on a side, centered on the star, from the shortest (14 s) exposure. Lower left: the same image and scale, but intensity scaled to emphasize the faint outer nebulosity (D). Features very near the star that are believed to be real are identified by letters A, B, C. Lower right: the previous frame after subtraction of an image of a single star from another WFPC2 exposure taken in the same series. The white circle outlines the saturated central region. The diffraction spikes and much of the scattered light structure has thereby been cancelled, showing the underlying nebulosity.

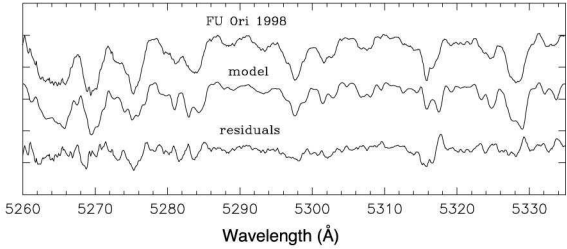


Fig. 16.— Comparison between the observed spectrum of FU Ori and the synthetic spectrum of the accretion disk model.

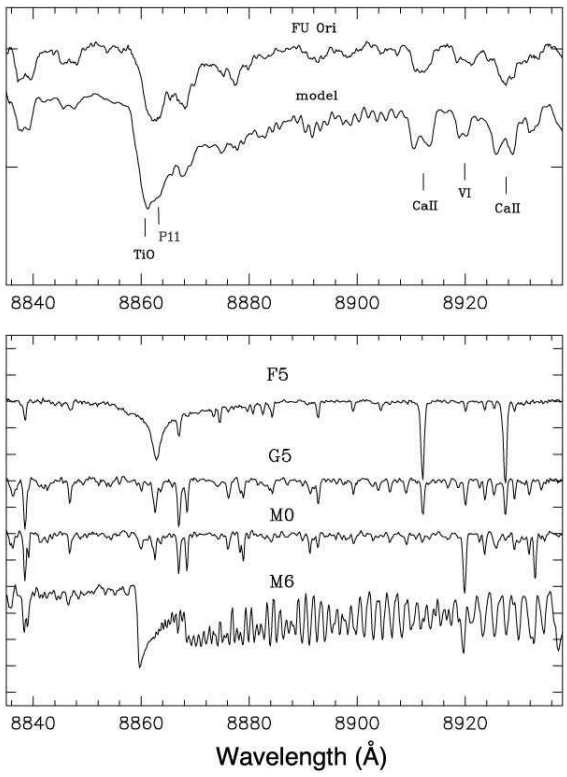


Fig. 17.— Upper panel: Comparison between the spectrum of FU Ori and the synthetic spectrum of the accretion disk model for the region of the TiO band and the IR Ca II lines. Lower panel: examples of the template spectra used in calculations of the accretion disk spectrum.

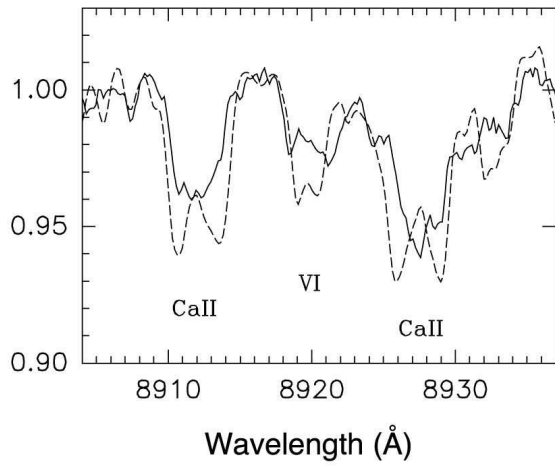


Fig. 18.— As Fig. 17 but for the region of the IR Ca II lines. Solid line: observed spectrum of FU Ori. Dotted line: synthetic spectrum of the accretion disk. Note the differences in the line widths and profiles.

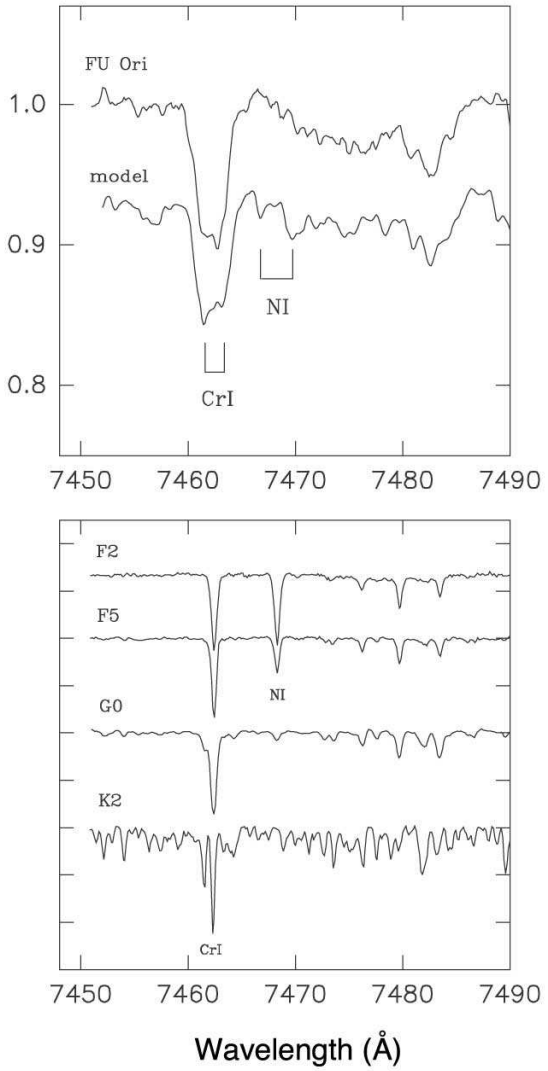


Fig. 19.— As Fig. 17: the line of N I ( $EP = 7$  eV) which should be split by the fast rotation of the inner disk is not present in the observed spectrum of FU Ori.

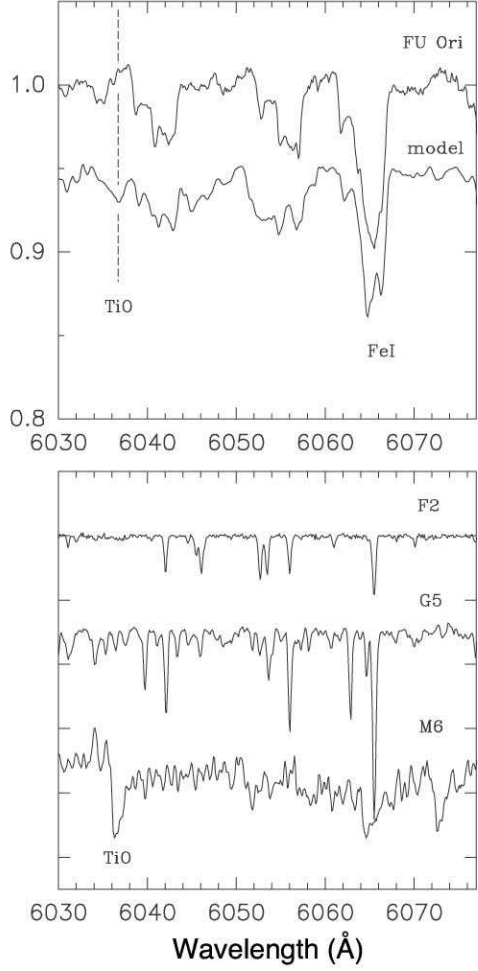


Fig. 20.— As Fig. 17: the ScO/TiO feature predicted by the accretion disk model is absent in the observed spectrum of FU Ori.

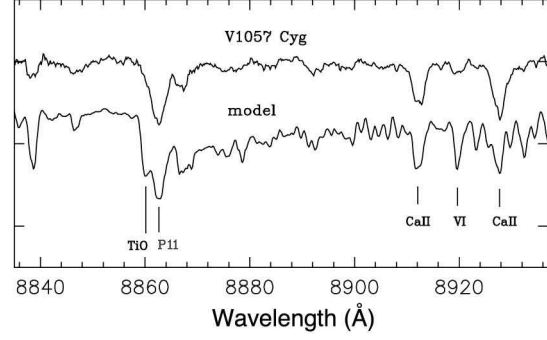


Fig. 21.— The same as Fig. 17 but for V1057 Cyg, an average of the SOFIN spectra of 1998, 1999, and 2000 when TiO was not present in the shell. Note the absence of the TiO feature in the observed stellar spectrum.

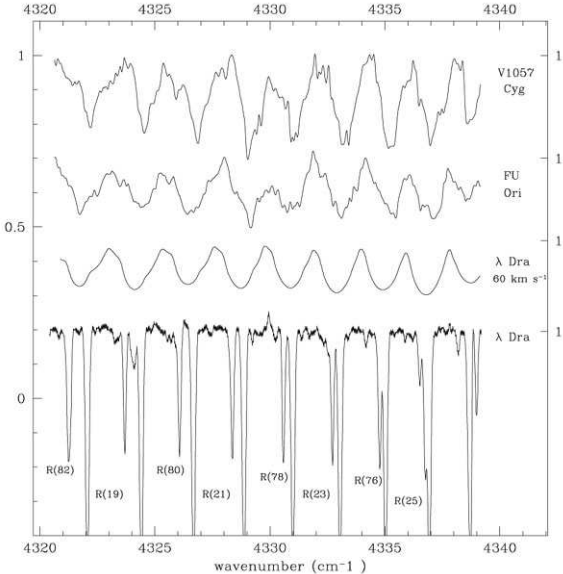


Fig. 22.— At top: the spectra of V1057 Cyg and FU Ori in the  $2.3\ \mu\text{m}$  region, as observed by K. Hinkle on 1999 October 24. They have been smoothed by a 5-pixel box and corrected for their nominal optical-region velocities. The FTS spectrum of  $\lambda$  Dra (M0 III) from the atlas of Wallace & Hinkle (1996) has been slightly smoothed (bottom) and spun up to  $v_{\text{eq}} \sin i = 60\ \text{km s}^{-1}$  (above).

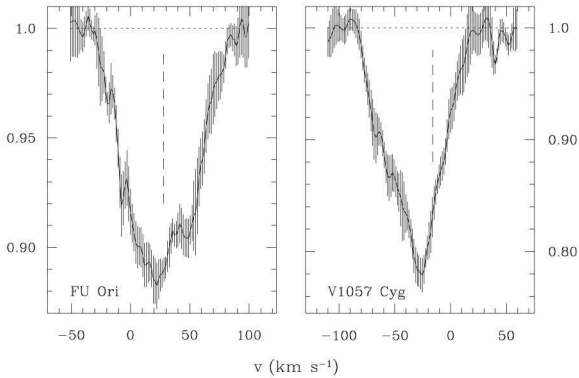


Fig. 23.— Mean CO profiles for V1057 Cyg (average of 5 lines) and FU Ori (4 lines). The vertical solid lines show the  $\pm 1$  standard deviations of each mean point. The vertical dashed line indicates the optical velocity of each star.

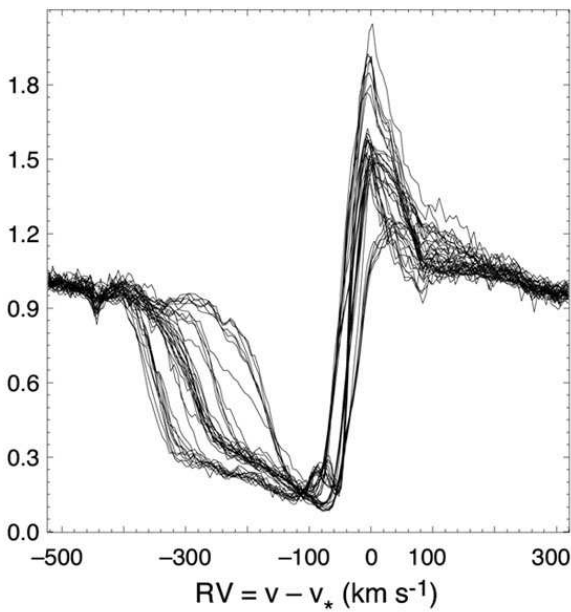


Fig. 24.— Variations of the H $\alpha$  profile of V1057 Cyg in 1996–2001.

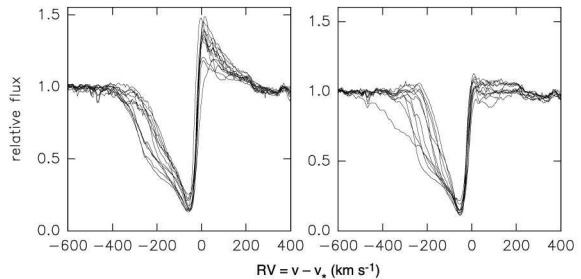


Fig. 25.— Variations of the H $\alpha$  profiles of FU Ori in 1995–2000. Left panel: all profiles having the emission peak intensity (in continuum units) greater than 1.20. Right panel: all those having peak intensity less than 1.10. These illustrate how the longward emission peak is suppressed to different degrees on different occasions. The extension of the P Cyg absorption wing to different negative velocities is also apparent. There is no obvious correlation between the two.

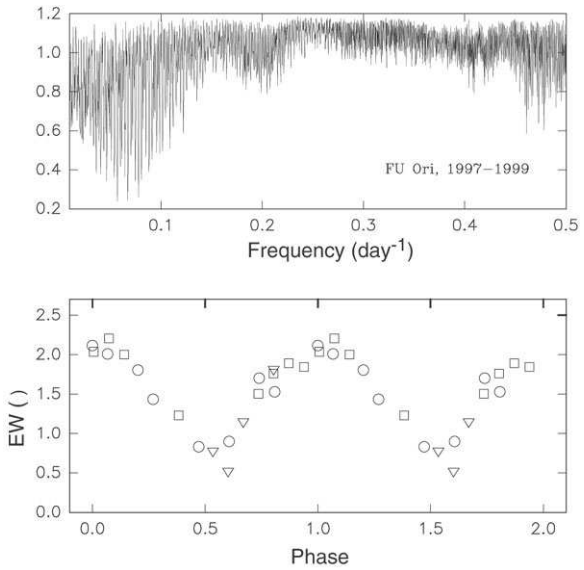


Fig. 26.— Upper panel: periodogram of the variation of EW of the “fast wind” section of H $\alpha$  in FU Ori for a period range of 2 to 100 days. Lower panel: phase diagram for a period of 14.847 days. Circles: data of 1997; squares: data of 1998; triangles: data of 1999.

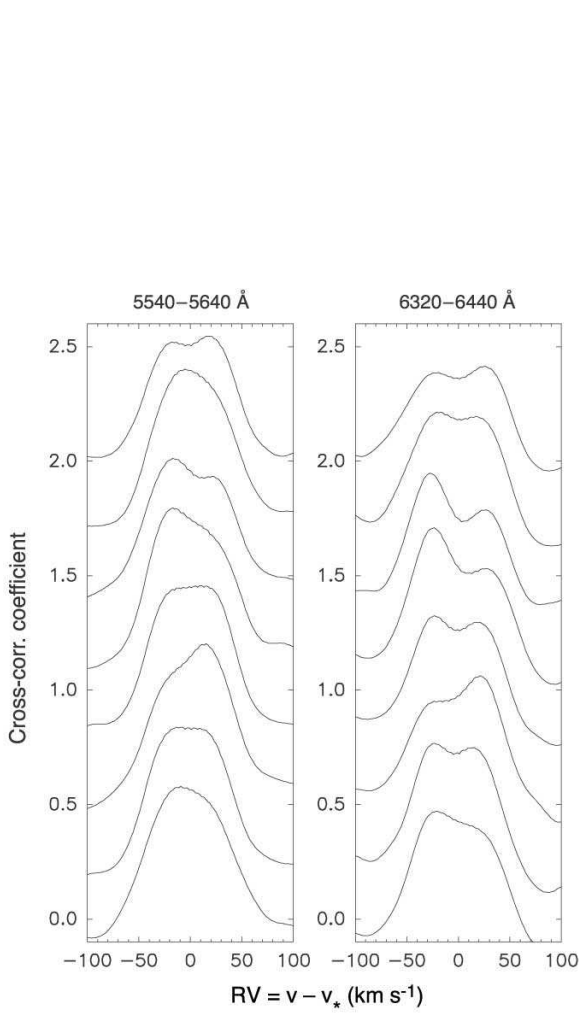


Fig. 27.— Cross-correlation functions, showing night-to-night variability in the photospheric line profiles in V1057 Cyg over 8 consecutive nights of August 1997.

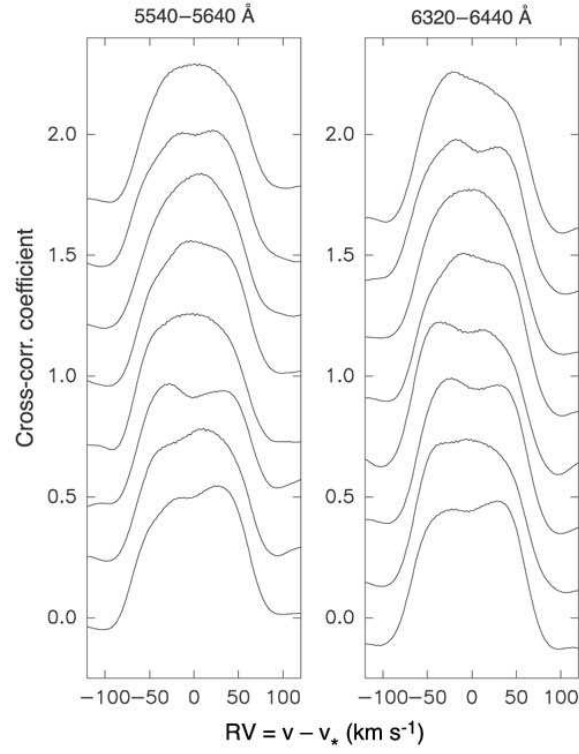


Fig. 28.— Cross-correlation functions, showing night-to-night variability in the photospheric line profiles in FU Ori in December 1997.

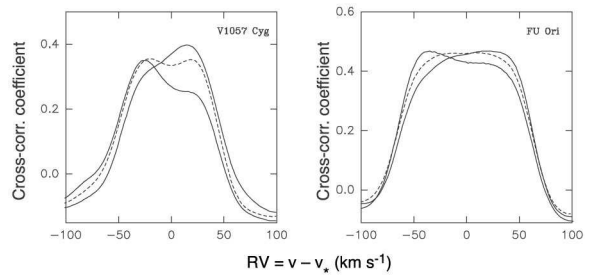


Fig. 29.— Three cross-correlation functions, showing the typical variations of the photospheric line profiles in V1057 Cyg and FU Ori: the blue-shifted, centered, and red-shifted profiles.

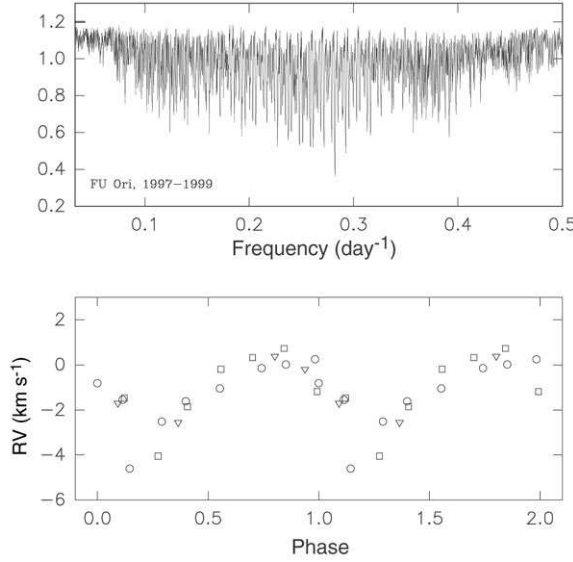


Fig. 30.— Upper panel: radial velocity periodogram for FU Ori in 1997–1999, for a period range from 2 to 30 days. The most probable period is about 3.543 days; Lower panel: phase diagram for the period of 3.543 days; circles: data of 1997; squares: data of 1998; triangles: data of 1999.

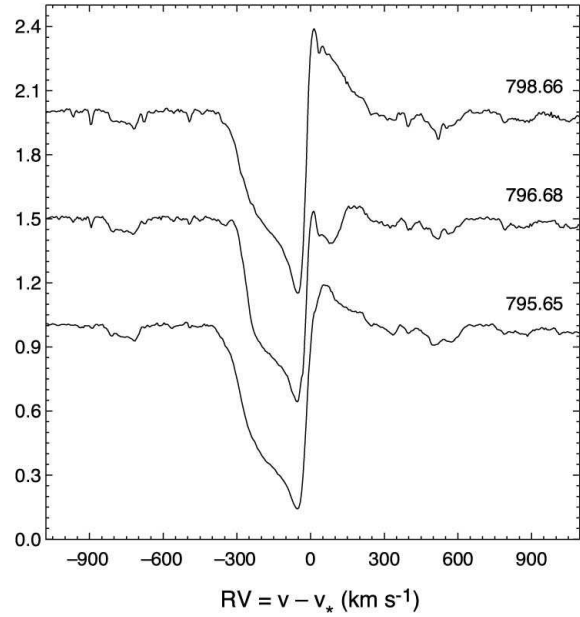


Fig. 31.— Three SOFIN spectra of the H $\alpha$  region of FU Ori, obtained on the dates indicated (which are JD - 2450000.) The absorption component at about  $RV = +90 \text{ km s}^{-1}$  in the longward wing of H $\alpha$  was present on the middle date, but not on the day before or two days later.

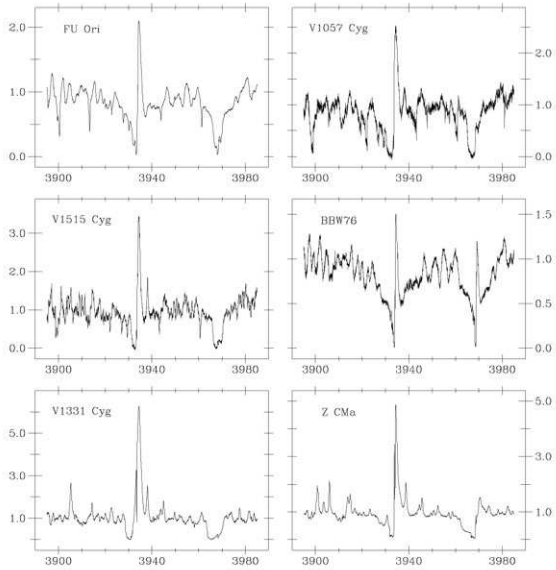


Fig. 32.— The region of the Ca II H and K lines in six stars, among them three classical FUors, as observed with HIRES on 1998 October 30, 31. The narrow emission line closely longward of  $\lambda 3933$  in several objects is Fe II  $\lambda 3938.29$  [RMT 3].

TABLE 1  
 $\text{H}\alpha$  STRUCTURE IN V1057 CYG

Source	Date	Absorption		Emission		
		EW (Å)	$A_c$	EW (Å)	$E_c$	$V$ mag.
BM	1981 Jun 23	1.86	0.41, 0.40	0.77	0.19	11.2
BM	1982 May 15	0.24+0.24	0.15, 0.21	1.00	0.27	11.35
BM	1982 Jul 12	1.36	0.55, 0.13	0.99	0.22	11.35
BM	1982 Jul 13	1.40	0.55, 0.14	0.95	0.22:	11.35
C	1984 Oct 10	2.24+0.84	0.59, 0.56	0.96	0.35	11.5
C	1984 Dec 6	3.44	0.52	0.91	0.58:	11.5
Lick	1985 Sep 23	4.2	0.66	0.62	0.28	11.6
C	1985 Nov 24	0.14+1.60	0.32, 0.55	1.79	0.93	11.6
Budge	1988 Aug 25	7.3	0.69	0.65	0.34	11.6
Welty	1988 Nov 30	7.6	0.70	2.2	0.92	11.6
HC	1992 Dec 7	5.8	0.90	...	0.04	11.6
SOFIN	1996 Oct 30	3.52	0.89	0.96	0.45	12.35
HIRES	1997 Aug 13	4.24	0.87	1.03	0.51	12.45
SOFIN	1997 Aug 15–22	4.28	0.88	1.13	0.56	12.45
SOFIN	1998 July 2–15	4.01	0.84	1.66	0.83	12.95
SOFIN	1999 Jul 23–Aug 3	5.31	0.86	0.60	0.52	12.82
SOFIN	2000 Aug 7–10	3.57	0.86	1.23	0.51	12.59
SOFIN	2001 Jul 29–Aug 9	3.26	0.92	0.44	0.22	12.5
HIRES	2002 Dec 16	3.06	0.84	1.71	0.62	12.5

NOTE.— Col.1: the source abbreviations are:

BM: Bastien & Mundt 1985

C : Croswell et al. 1987

Lick, unpublished; low resolution ( $\approx 5200$ )

Budge, unpublished; Palomar 60-inch, echelle

Welty et al. 1992

HC: Hartmann & Calvet 1995

SOFIN: Nordic Optical Telescope, this paper

HIRES: Keck I, this paper

Cols. 3 and 5: EW in the equivalent width of the feature

Col.5:  $A_c$  is here the central depth of the deepest point in the absorption line, measured downward from the continuum, in continuum units

Col.7:  $E_c$  is here the central height of the emission peak, measured upward from the continuum, in continuum units. It is subject to rapid night-to-night variations: see §4.4.1

TABLE 2  
SHELL LINE STRUCTURE IN V1057 CYG

	$v$ (km s $^{-1}$ )	$\tau_0$ (km s $^{-1}$ )	$\sigma$ (km s $^{-1}$ )	EW (mÅ)		$v$ (km s $^{-1}$ )	$\tau_0$ (km s $^{-1}$ )	$\sigma$ (km s $^{-1}$ )	EW (mÅ)		$v$ (km s $^{-1}$ )	$\tau_0$ (km s $^{-1}$ )	$\sigma$ (km s $^{-1}$ )	EW (mÅ)	
	Ti I [5] 4997.099					Ti I [38] 4999.504					Ba II [2] 6496.896				
1	...	...	...	...		-128.	0.08	3.9	13.		-128.	0.23	8.3	96.	
2	-107.	0.022:	5.4:	5.:		-107.5	0.27	5.1	53.		-107.	0.27	6.5	86.	
3	-90.	0.26	3.6	36.		-88.5	0.87	6.0	165.		-92.5	0.33	5.5	89.	
4	-78.	0.33	4.5	56.		-78.	1.17	6.0	202.		-80.	0.82	7.8	267.	
5	-59.5	0.27	4.8	49.		-61.5	1.77	5.1	221.		-61.	1.06	6.5	265.	
	Li I [1] 6707.81					Rb I [1] 7800.227					Rb I [1] 7947.60				
1	-128.	0.17	8.0	72.		-129.	0.075	6.9	33.		-126.	0.078	4.9	25.	
2	-104.	0.31	8.7	136.		-106.	0.085	7.7	41.		-100.	0.065	4.9	21.	
3	...	...	...	...		...	...	...	...		...	...	...	...	
4	-82.	0.96	8.3	326.		-79.5	0.32	10.	194.		-81.	0.21	9.8	127.	
5	-60.5	1.29	8.0	389.		-58.5	0.52	4.6	131.		-60.	0.32	5.3	101.	

NOTE.— The symbols are:  $v$  is the central (heliocentric) velocity of that component;  $\tau_0$  is its central optical thickness and  $\sigma$  is its width, both expressed as gaussian parameters as explained in the text; EW is its equivalent width.

TABLE 3  
Ti I SHELL LINE STRUCTURE, 1997 AUG. 12, 13

Component (km s $^{-1}$ )	$\xi_0$ (km s $^{-1}$ )	T <sub>exc</sub> (°K)	log N(Ti I) (cm $^{-2}$ )
-128	1.3:	4000.:	13.38:
-107	1.9	4350.	14.08
-89	3.1	3650.	14.78
-78	4.7	3600.	15.05
-61	4.8	3700.	14.95

TABLE 4  
EQUIVALENT WIDTHS (IN Å) OF EMISSION CORES

Date	$V$	Fe I 5615	Fe I 6191	Fe I 6393	Fe I 6400	Fe II 6516
1996 Oct	12.35	0.154	...	0.156	0.236	0.210
1997 Aug	12.45	0.237	0.310	0.220	0.319	0.266
1998 Jul	12.95	0.205	0.306	0.175	0.268	0.226
1999 Jul	12.82	0.179	0.285	0.190	0.246	0.180
2000 Aug	12.58	0.192	0.291	0.170	0.256	0.239
2001 Aug	12.48	0.260	0.240	0.200	0.271	0.245

TABLE 5  
TEMPLATE STARS

Star	MK Type
32 Aql	F2 Ib
41 Cyg	F5 II
$\beta$ Aqr	G0 Ib
9 Peg	G5 Ib
40 Peg	G8 II
43 Tau	K2 III
$\beta$ And	M0 IIIa
72 Leo	M3 Iab-Ib
30 Her	M6 IIIa

TABLE 6  
FLUX CONTRIBUTIONS TO DISK

Type	5500 Å	6400 Å	9000 Å
F2-F7:	0.5	0.4	0.3
F8-K2:	0.4	0.4	0.35
K5-M6:	0.1	0.2	0.35
total:	1.0	1.0	1.0

TABLE 7  
FITS TO THE CO LINES

Star	Component	$v_{\text{eq}} \sin i$ (km s $^{-1}$ )	$v$ (km s $^{-1}$ )	$A_c$
V1057 Cyg	1	12.	-26.	0.085
	2	45.	-35.	0.15
FU Ori	1	48.	+27.	0.105

NOTE.— $A_c$  is defined in Table 1.

TABLE 8  
EWs OF  $H\alpha$  P CYG ABSORPTION IN FU ORI

JD-2450000	EW (Å)	JD-2450000	EW (Å)
0054.539	1.478	1092.721	2.035
0055.575	1.177	1093.704	2.206
0795.647	2.114	1094.713	1.999
0796.676	2.007	1471.693	0.774
0798.665	1.805	1472.722	0.516
0799.706	1.432	1473.689	1.144
0802.678	0.831	1475.717	1.808
0804.697	0.897	1887.569	1.231
0806.678	1.701	1888.527	1.133
0807.695	1.530	1889.571	1.745
0890.399	1.229	1890.572	1.000
1088.672	1.504	1892.573	1.308
1089.706	1.759	1893.568	1.308
1090.704	1.890	1896.572	0.755
1091.706	1.843	...	...

NOTE.— The equivalent widths are for the section of the absorption line between  $RV = -110$  and  $-270 \text{ km s}^{-1}$

TABLE 9  
RADIAL VELOCITIES FROM CROSS-CORRELATION FUNCTIONS

V1057 Cyg		FU Ori	
JD-2450000	RV (km s <sup>-1</sup> )	JD-2450000	RV (km s <sup>-1</sup> )
387.448	-1.590	54.538	1.139
676.572	-1.067	55.575	0.461
677.398	-2.746	795.647	-0.800
678.402	3.270	796.676	-2.501
679.395	-0.386	798.665	0.029
680.384	-4.435	799.705	-4.599
681.384	-6.608	802.677	0.256
682.383	-1.637	804.697	-1.040
683.405	1.017	806.678	-1.536
997.472	4.266	807.694	-1.601
999.601	-10.106	890.398	-0.140
1000.562	-1.914	1088.672	0.330
1002.532	0.967	1089.706	-1.186
1003.546	-8.107	1090.703	-4.049
1005.521	-5.065	1091.706	-0.190
1008.545	-0.917	1092.721	0.730
1383.554	1.829	1093.704	-1.470
1384.603	-2.308	1094.713	-1.849
1385.556	-10.181	1471.693	0.371
1386.550	5.770	1472.722	-1.709
1387.515	0.604	1473.689	-2.569
1388.529	1.606	1475.717	-0.206
1389.522	-8.802	1887.569	-0.369
1390.555	-0.839	1888.527	-1.780
1391.524	0.689	1889.571	1.290
1392.552	2.195	1890.572	3.721
1393.586	-3.338	1892.573	1.160
1394.561	-4.708	1893.568	-0.624
1764.606	4.634	1896.572	-1.344
1765.611	2.115	...	...
1766.599	3.804	...	...
1767.609	9.921	...	...
2120.480	-0.997	...	...
2121.493	1.509	...	...
2123.571	3.578	...	...
2124.495	-2.060	...	...
2125.540	-2.953	...	...
2127.595	2.997	...	...
2128.557	-3.084	...	...
2129.584	0.271	...	...

TABLE 9—*Continued*

V1057 Cyg		FU Ori	
JD-2450000	RV (km s <sup>-1</sup> )	JD-2450000	RV (km s <sup>-1</sup> )
2130.568	−1.492	...	...
2131.501	−1.674	...	...

NOTE.—RV is the measured radial velocity minus the radial velocity of the star: −16 km s<sup>−1</sup> for V1057 Cyg and +28 km s<sup>−1</sup> for FU Ori.